THE FLORIDA STATE UNIVERSITY

COLLEGE OF ARTS AND SCIENCES

CHARACTERIZING THE VARIABILITY OF THE INDIAN MONSOON:

CHANGES IN EVAPORATIVE SOURCES FOR SUMMERTIME RAINFALL EVENTS

By

PETER PANTINA

A Thesis submitted to the
Department of Earth, Ocean, and Atmospheric Science
in partial fulfillment of the
requirements for the degree of
Master of Science

Degree Awarded:
Spring Semester, 2010

The members of the committee approve the thesis of Peter Pantina defended on December 7, 2010.

_____

Vasubandhu Misra
Professor Directing Thesis

_____

Sharon Nicholson
Committee Member

_____

Paul Ruscher
Committee Member

The Office of Graduate Studies has verified and approved the above named committee members.

I dedicate this to...

ACKNOWLEDGEMENTS

I would like to acknowledge Dr. Vasu Misra who encouraged me to conduct this research and offered much guidance along with way. I would also like to thank Dr. Sharon Nicholson for invoking my initial research interests, Dr. Paul Ruscher for giving me the opportunity to teach and learn from others, and both for agreeing to be on my committee. Dr. Steven Chan at COAPS contributed invaluably to my progression as a programmer, and his help was extremely appreciated throughout this process. Doug Klotter taught me some initial programming techniques that allowed me to start down the path of research. My family provided encouragement when I lost it from time to time, and my friends at FSU made my time outside the office enjoyable and memorable, and they are greatly appreciated.

TABLE OF CONTENTS

LIST OF TABLES

LIST OF FIGURES

ABSTRACT

This study focuses on the interannual and intraseasonal variability of evaporative sources for rainfall events during the Indian monsoon. The monsoon is an important part of the economy and lifestyle in India, thus, any improvements in our understanding of its mechanisms would be directly beneficial to society. We first discuss the use of evaporative sources of rainfall events as an important tool to help increase our knowledge of the variations of the monsoon. We then outline the variability of the monsoon on an interannual (wet and dry years) and intraseasonal (active and break periods) time scale. We use three reanalyses (NCEP-R2, CFSR, and MERRA) and an IMD gridded rainfall dataset to trace the location and strength of evaporative sources via a quasi-isentropic back trajectory program. The program using reanalysis winds and evaporation, among other parameters, to estimate these sources back in time. We discuss the differences in parameters between the datasets on a seasonal, interannual, and intraseasonal time scale. We then thoroughly investigate the strength and location of evaporative sources between datasets on interannual and intraseasonal time scales, and we attempt to explain the variations by analyzing the differences in the input parameters and circulation mechanisms themselves.

The study finds that the evaporative sources for given interannual or intraseasonal rainfall events do vary in strength and location. Interannually, the strongest change in evaporative source occurs over central India and the Arabian Sea, suggesting that the overall monsoon flow contributes moisture for Indian rainfall on this time scale. Intraseasonally, the strongest change in evaporative source occurs over the Bay of Bengal, suggesting that landfalling tropical cyclones contribute moisture for Indian rainfall on this time scale. All three reanalyses yield similar fields of evaporative source. We conclude that accurate prediction of the Indian monsoon requires improved understanding of both interannual and intraseasonal oscillations since the sources of moisture for these events are unique.

CHAPTER ONE
INTRODUCTION

1.1 Background and motivation

The Indian monsoon is a summertime (June – September) phenomenon that features an annual reversal of the winds over India along with the occurrence of 75% to 90% of the country's annual precipitation (Mooley and Parthasarthy 1984). Because of its enormous contribution to total rainfall, the monsoon has widespread impacts on the Indian economy as well as on the robustness of a given year's agricultural yield (Krishnamurthy and Shukla 2000). Agricultural success is highly dependent on precipitation since crops are largely rain-fed across most of the country (Kerr 1996). Variability of the monsoon on interannual and intraseasonal time scales is a well-documented and common occurrence (Lawrence and Webster 2001; Goswami and Mohan 2001) and therefore has large implications for the population of India. Variability studies are necessary for improved understanding and prediction of the seasonal and intraseasonal changes in the monsoon's character.

Variability of the monsoon is driven by different mechanisms depending on the time scale of interest. Krishnamurthy and Shukla (2000) showed that the Indian monsoon is inherently difficult to predict for this reason. They concluded that seasonal mean rainfall over India is influenced by seasonally persisting, externally forced conditions as well as subseasonal, fluctuating oscillations that differ in spatial character (Figure 1-1). Goswami and Mohan (2001) used outgoing longwave radiation (OLR) and described the intraseasonal oscillations as chaotic and unpredictable. They suggested that overall monsoon predictability depends on the influence of the intraseasonal fluctuations on the seasonal mean and found the influence to be non-negligible. If the monsoon were maintained only by external, slowly varying, boundary-forced conditions as outlined in Shukla (1998), its predictability would be considerably simpler than what we currently see. They showed that a tropical atmospheric circulation will evolve to the initial conditions set by ocean forcing, regardless of the initial atmospheric conditions. However, with regard to the Indian monsoon, the chaotic intraseasonal oscillations confound the ability to

predict its performance on the basis of the seasonally persistent component of variation or the nearby ocean conditions alone.

1.2 Evaporative sources

To improve the understanding of the mechanisms of Indian monsoon variability, we set out to quantify the changes in evaporative sources for the summertime precipitation events over India. In general, moisture sources are a good metric by which to study climate variability in the tropics. Mooley and Parthasarthy (1984) showed that in the tropics, temperature fluctuations do not vary enough to accurately study interannual or intraseasonal changes in climate patterns. However, they claimed that variability in evapotranspiration fields plays a large role in tropical climate patterns and should be used to document climate changes in low-latitude regions.

Evaporative source is defined as the source of water molecules for a given precipitation event over a region (Dirmeyer and Brubaker 1999). The sources of precipitation in a region originate from moisture already in the atmosphere over the region, convergence of atmospheric moisture advected into the region by winds, and evaporation of surface moisture into the atmosphere over the region, either from land or water (Trenberth 1999). Trenberth et al. (2003) explained that global evaporation rates are on the order of five mm day^{-1} during the summer and that they partly contribute to precipitation. However, convergence of moisture from remote location explains the source of moisture for moderate and heavy precipitation events that commonly exceed this local rate of evaporation. Trenberth et al. (2003) concluded that moisture already in place over a given precipitation event contributes little to overall moisture source, and that the largest contributors to moisture source are evaporation and remote advection. Figure 1-1 illustrates the overall contribution of remote advection and local evaporation to precipitation events over a region.

1.2.1 Evaporation and soil moisture

In their study, Dirmeyer and Brubaker (1999) assumed that evaporation contributes to overall rainfall and that soil moisture controls evaporation. They concluded that rainfall is therefore a direct function of soil moisture. The assumption that soil moisture controls evaporation is a valid one used by others in the literature, including Trenberth (1999), who stated that local evaporation was dictated by surface or soil moisture and used that assumption to characterize the local and remote influences of moisture over different regions. Dirmeyer and Brubaker (1999) also

claimed that soil moisture acts as a source of water for precipitation and can change the thermodynamics as well as the atmospheric circulation of a given state. Indeed, Paegle et al. (1996) showed that evaporation influences jets and convergence patterns over the United States more so than precipitation itself. Koster et al. (2004) reported that soil moisture can influence weather through its impact on surface fluxes, and that oceanic or boundary-forced impacts on precipitation are relatively small compared to the impacts of soil moisture on precipitation.

Over India, soil moisture controls much of the climate patterns that dominant the region. Koster et al. (2004) discovered regions of the globe where land atmosphere coupling strength reveals "hot spots," or regions where the atmosphere responds strongly to land surface conditions and changes within those parameters. India was considered to be such a region in their study, which suggests that monitoring of soil moisture within the region will yield improved seasonal forecasting, especially of local precipitation events. Dirmeyer (1999) completed a study in which he ran climate models with and without a high-quality, global soil wetness dataset. He concluded that improved soil wetness leads to an enhancement in the simulation of precipitation, particularly over the monsoon region of southern Asia. Finally, Arpe et al. (1998) completed a study of model sensitivity to boundary-forcing conditions over India. They concluded that inclusion of realistic soil moisture into a 90-day forecast of monsoon circulation over India improves the skill of precipitation forecasts over that region.

1.2.2 Remote Advection

Moisture sources are not limited to local evaporation processes. Advection of moisture from nearby landmasses or ocean basins by winds is equally important in contributing to moisture for precipitation. Brubaker et al. (1993) cited Benton et al. (1950) and their conclusion that water vapor from the oceans could pass over continental regions without immediately raining out as precipitation. Budyko (1974) concluded that a majority of precipitation is generated from moisture of "external origin" rather than of local origin. Evaporation off the oceans is a large component here, as the surface of the oceans is always wet and moisture is unlimited (Trenberth 1999). However, remote land regions also contribute to externally-originating moisture, as upstream evaporation over the surface creates atmospheric moisture that may be advected by winds (Brubaker et al. 1993). Trenberth and Guillemot (1998) claimed that this terrestrial- and marine-based atmospheric moisture either flows past a region or converges over it and precipitates out; the mechanism depends on the dynamics of the circulation.

In India, remote advection largely impacts the moisture that enters the region. In their study, Cadet and Reverdin (1981) found that the onset of the Indian monsoon is associated with cross-equatorial water vapor transport passing from eastern Africa, over the Arabian Sea, and across to India. They concluded that 70% of the moisture passing over the western coast of India originates from the southern hemisphere, and that the remaining moisture advects in from the Arabian Sea along the path of the cross-equatorial flow. Likewise, Lim et al. (2002) isolated two main regions of moisture over southern Asia in their study of the seasonal cycle of the Asian monsoon. They showed that a continuous supply of moisture from the Indian Ocean as well as the western Pacific Ocean sustain the seasonal monsoon rainfall events that occur during the boreal summer. The source over the Indian Ocean is the persistent supplier of moisture over India, whereas the western Pacific source plays a role in the East Asian monsoon (not discussed here). Low-level moisture convergence transport into the Indian region makes the atmosphere unstable and results in the development of convective instability and subsequent monsoon rainfall.

1.2.3 Tracing evaporative sources

Since Indian monsoon rainfall is largely dictated by contributions of moisture from evaporation, soil moisture, and remote advection, tracing evaporative sources for summertime rainfall events will help improve the understanding of monsoon variability. In fact, Trenberth et al. (2003) stated that tracking the movement of moisture serves to elucidate the large-scale circulation patterns that bring moisture to a given region. We assume that isolating evaporative sources using back trajectories will help us infer source regions and help explain if proposed mechanisms for monsoon variability are responsible for the variation in rainfall that we observe. In their study, Dirmeyer and Brubaker (1999) set out to answer two important questions:

1. What moisture sources dominate the precipitation patterns?
2. What is the magnitude and character of interannual and intraseasonal variability in moisture sources and sinks [precipitation]?

We attempt to answer these same questions and assess whether there is interannual or intraseasonal variability in these evaporative sources with the goal of elucidating a portion of the total variability of the monsoon.

Past studies by Dirmeyer and Brubaker (1999) found significant interannual variation in the evaporative sources over the Midwest U.S. during drought and flood years. They found

variability in the spatial layout of evaporative sources from year to year and also isolated differences in the ratios of local to remote evaporative contribute to total atmospheric moisture over the region. Chan and Misra (2009) also found a significant different in interannual evaporative source over the southeastern U.S. using a similar technique. They discovered that wet boreal summers feature remote evaporation that is advected from the ocean, whereas dry boreal summers feature more localized evaporative sources originating closer to the U.S. However, they concluded that anomalous wet events feature evaporative sources that are not significantly different in wet or dry years, suggesting no interannual variation of subseasonal precipitation events. We subsequently characterize the variability of moisture sources, if any, over the Indian region to note any changes in character of moisture source over the region.

1.3 Monsoon variability

1.3.1 Interannual variability

As mentioned earlier, interannual monsoon variability is a well-known phenomenon. The standard deviation of seasonal monsoon rainfall is only about 10% of the mean (Gadgil 2003), yet this is sufficient to have years often labeled as "flood" or "drought" in the literature because of the significant impact on agriculture (Krishnamurthy and Shukla 2000). Using empirical orthogonal function (EOF) analysis, Krishnamurthy and Shukla (2000) demonstrated that drought or flood years are characterized by rainfall anomalies of the same sign over most of the Indian region (Figure 1-2a). Therefore, wet years feature a countrywide increase in rainfall over the monsoon season, whereas dry years feature a countrywide reduction in rainfall. Additionally, the interannual variation of rainfall over India is nonperiodic (Krishnamurthy and Kinter 2003), such that dry years do not immediately precede or follow wet years. Several proposed mechanisms of variability are discussed below.

The El Niño Southern Oscillation (ENSO) plays a significant role in maintaining interannual variability of the monsoon. In their study, Krishna Kumar et al. (1999) suggested that there is an inverse relationship between the seasonal rainfall over India and the summertime phase of ENSO. A weak monsoon occurs along with a developing warm ENSO event, whereas a strong monsoon occurs along with a developing cold ENSO event. During a warm ENSO, the tropical Walker circulation shifts toward the east; the rising limb moves over the eastern Pacific warm pool and the sinking limb moves over India. Subsidence and drier air over the country

leads to a drought during the summertime. In similar studies, Krishnamurthy and Kinter (2003) and Kirtman and Shukla (2000) discovered that this inverse correlation peaks in the October through January period following the monsoon season.

Another proposed mechanism of monsoon interannual variability is the tropical biennial oscillation (TBO). As outlined by Meehl (1994) and Meehl (1997), the TBO is a series of changes in the ocean surface and atmospheric circulation over southern Asia and the western Pacific. The oscillation starts with anomalously warm SSTs in the central Indian Ocean during a winter prior to a monsoon season. These anomalies persist into the following summer because of the memory effects of the ocean described in the study. The persistent warm SSTs lead to enhanced monsoon rainfall that season due to an increase in land-sea temperature contrast. Accompanying the strong monsoon are increased mixing and evaporation due to winds over the ocean and subsequent cooling of the waters. The cool temperature anomalies persist through the following winter and summer, and a weak monsoon is experienced in India during the next season. This coupled air-sea interaction peaks every two years and helps explain some of the changes in annual monsoon rainfall (Krishnamurthy and Kinter2003), but Fasullo (2004) concluded it is often confounded by changes in the phase of ENSO.

Furthermore, changes in snow cover over Eurasia have been shown to affect the interannual variability of the monsoon. According to Bamzai and Shukla (1999), there is a significant inverse correlation between the amount of wintertime snow cover over western Eurasia and the following summer's rainfall over India. The mechanism is described by several authors, including Vernekar et al. (1995). They suggested that above-average amounts of snow and increased soil moisture over the Tibetan plateau funnel the energy from springtime incoming solar radiation toward melting the snow instead of increasing the temperature of the otherwise exposed land surface. The subsequent reduction in sensible heat flux over land reduces the temperature gradient from the ocean to the land and thereby reduces the overall monsoon circulation.

1.3.2 Intraseasonal variability

Intraseasonal variability explains the other, more chaotic component of seasonal monsoon rainfall totals. The variation in daily rainfall anomalies is some 50 to 100 times greater than the variation of rainfall from year to year (Krishnamurthy and Shukla 2000). In their study, Krishnamurthy and Shukla (2000) used EOF analysis to isolate the major mode of intraseasonal

variation and found that anomalies of one sign exist over most of central India and opposite-signed anomalies exist over the northern plains and far western India (Figure 1-2b). They identified these variations as “active” (“break”) periods, during which increased (decreased) rainfall occurs for a period of days over central (northern and southern) India (Figure 1-3). The length of a given active or break spell is not official and ranges from a few days (Krishnamurthy and Kinter 2003) up to 60 days (Suhas and Goswami 2008).

Krishnamurthy and Shukla (2006) broke the intraseasonal variability into two components: a 45-day oscillation that moves north and east, and a 20-day oscillation that moves north and west. Goswami and Mohan (2001) elaborated on the 45-mode in their study. They stated that summertime intraseasonal oscillations (ISO) result from a fluctuation in the tropical convergence zone (TCZ) between two regions. The northern region is over the monsoon trough, an area of low pressure that extends west to east from northwestern India to the Bay of Bengal. The atmospheric conditions associated with this positions result in convergence of atmospheric moisture and increased rainfall over India. The TCZ enhances the monsoon circulation in this position. When it moves toward the south, over the equatorial ocean away from the trough, the monsoon flow is weakened and a break in rainfall is observed.

Krishnamurthy and Shukla (2006) attributed most of the 20-mode activity to the passage of tropical cyclones over India from the Bay of Bengal. Many studies have found a high correlation with the activity of tropical cyclones across the northern Indian Ocean and the intraseasonal monsoon oscillations (Krishnamurthy and Shukla 2006; Goswami et al. 2003; Goswami et al. 2008). During active periods, the number of days when a low pressure system (LPS) is recorded in the Indian monsoon region increases dramatically, up to seven times that of a break period (Krishnamurthy and Shukla 2006). This is countered by a significant decrease in the amount of LPSs recorded during monsoon break periods (Figure 1-5). This result suggests that tropical cyclone activity plays an important role in maintaining the subseasonal variation of monsoon rains.

Figure 1-6 illustrates the overall contributions of mechanisms from various time scales to the monsoon climate system.

1.3.3 Interannual variation of intraseasonal oscillations

There is substantial debate regarding the existence of interannual variability of the monsoon ISO. Goswami and Mohan (2001) formulated a hypothesis that the monsoon ISOs are directly related

to the seasonal strength of the monsoon. Thus, they expected a higher occurrence of active (break) periods during a strong (weak) monsoon, having assumed that these periods directly contribute to seasonal monsoon totals. They concluded that the probability density functions (PDFs) of ISO activity are asymmetric and different in wet and dry years, suggesting some validity in their initial hypothesis. In their study, Lawrence and Webster (2001) argued that ISO activity is inversely correlated to Indian monsoon rainfall activity. They did not consider PDFs, but claimed that when ISO activity is strong during the summer (i.e., several active and break periods in a given season), monsoon strength will be weak.

However, other studies provide counterarguments. Singh et al. (1992) concluded that there is no relationship between ISO activity and monsoon rainfall. Similarly, Jones et al. (2004) focused on intraseasonal oscillations in both ISO and the Madden-Julian Oscillation (MJO), a wintertime tropical intraseasonal oscillation, and found that there is no statistically significant difference in tropical intraseasonal activity of any sort from year to year. In this study, we will attempt to isolate interannual variability of the evaporative sources for intraseasonal rainfall events, but we do not assume a correlated or uncorrelated relationship between the two.

We detail the source and use of all datasets in Section 2 and then discuss methodology and techniques of the study in Section 3. Here we specifically discuss the quasi-isentropic back trajectory program that forms the core of our study and allows us to trace evaporative sources back in time. Section 4 details the results of the study by comparison of various parameters of the datasets themselves and then by discussion of interannual and intraseasonal variability of the evaporative source for monsoon rainfall events. Finally, Section 5 gives a summary and conclusions of the findings, followed by ideas for future work.

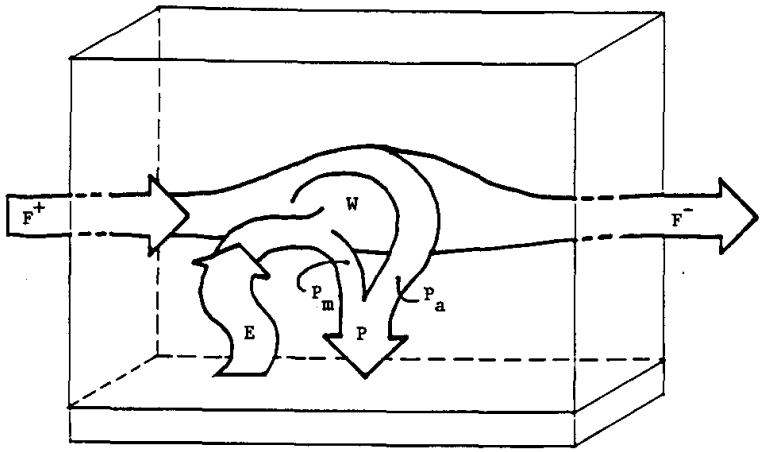

Figure 1-1. Diagram showing atmospheric moisture contribution over a land region. E represents local evaporation, P represents precipitation, and the F terms represent flux of moisture from the winds. P_a and P_m represent precipitation from advected and local moisture, respectively. From Brubaker et al. (1993).

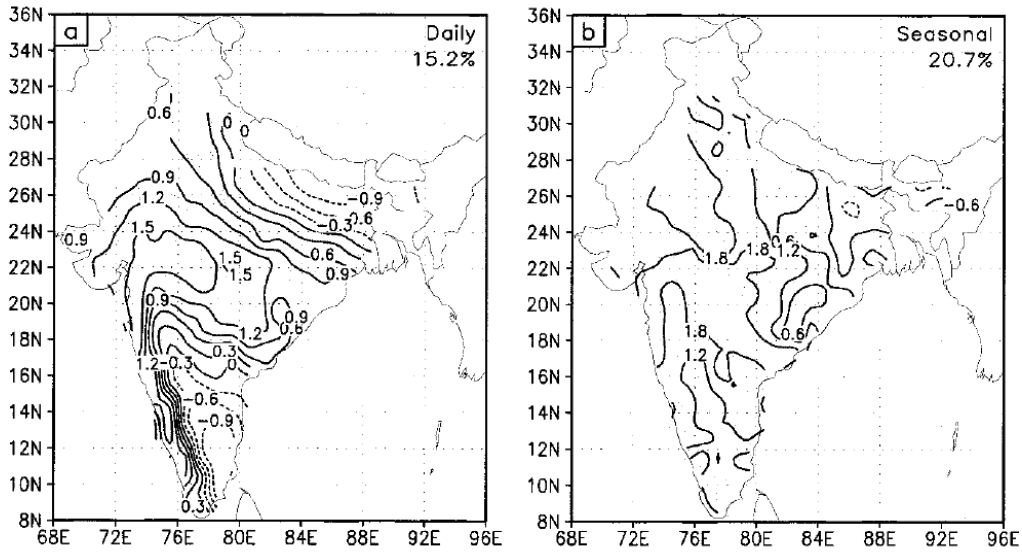

Figure 1-2. Plot showing the difference in EOFs of rainfall for daily (a) and seasonal (b) time scales over India. Sign differs across the country on a daily time scale and is of the same sign seasonally. From Krishnamurthy and Shukla (2000).

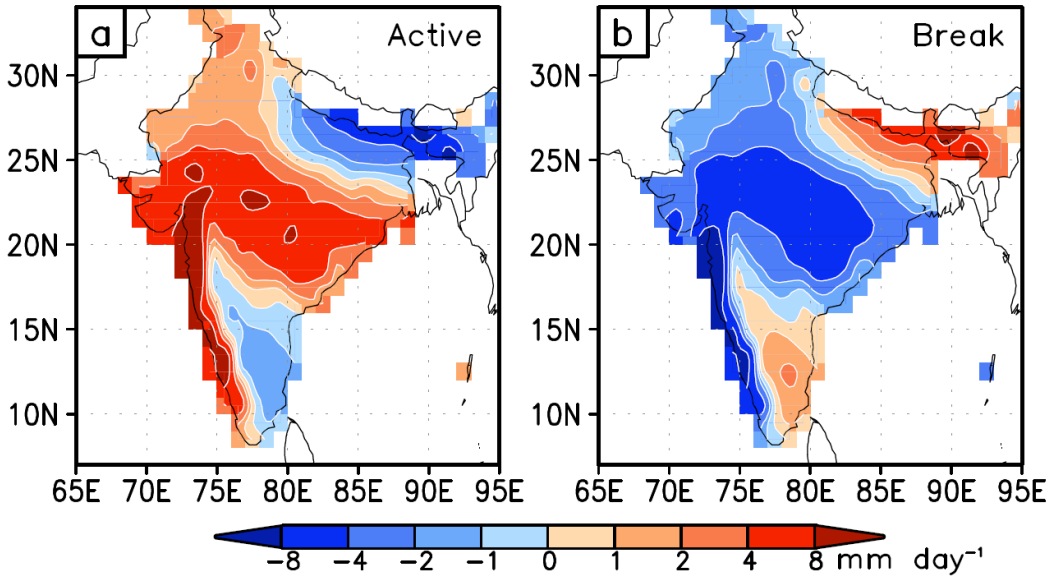

Figure 1-3. Active (a) versus break (b) composite rainfall anomalies. Active composites feature positive rainfall anomalies over central India and negative anomalies to the north and south. Break composites have the opposite pattern. From Krishnamurthy and Shukla (2006).

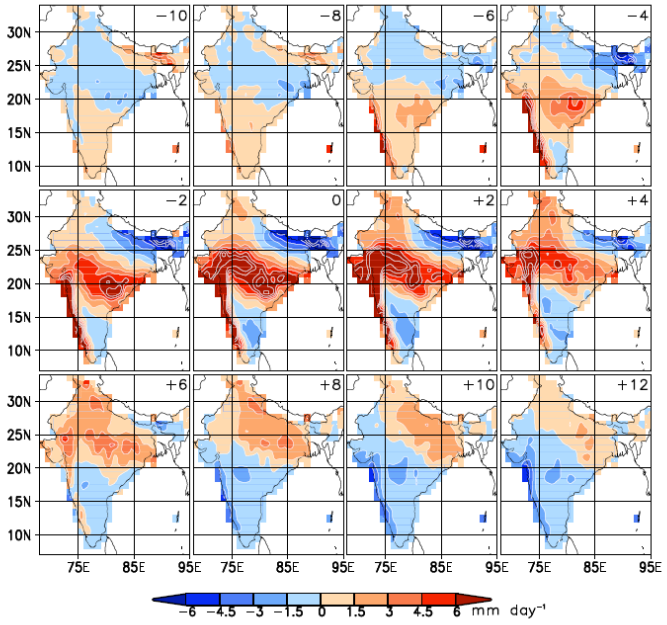

Figure 1-4. Plot showing the daily progression of the active and break phase across the country. From Krishnamurthy and Shukla (2006).

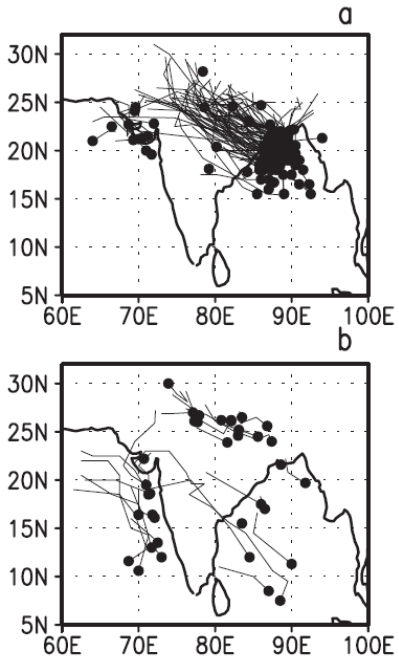

Figure 1-5. Plot showing the origin and tracks of LPSs during active phases (a) and (b) break phase composites of the monsoon. From Goswami and Mohan (2001).

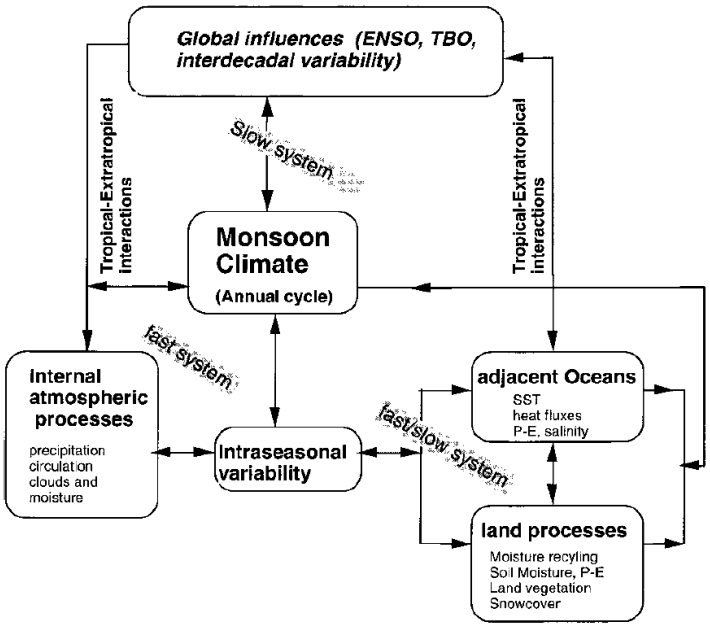

Figure 1-6. Diagram showing components and linkages of the monsoon system. In this study, we focus on the changes in monsoon climate due to global influences on an interannual scale (ENSO, TBO) and due to intraseasonal variability. Intraseasonal variability is dictated by internal atmospheric processes including rainfall, boundary conditions of the ocean, and land processes including soil moisture. From Lau et al (2000).

CHAPTER TWO
DATA

2.1 Precipitation

This study incorporates the Indian Meteorological Department (IMD) high-resolution daily gridded rainfall dataset over the Indian region. The dataset was originally created by Rajeevan et al. (2006) for their analysis of active and break spells during the Indian monsoon. It is an IMD rain-gauge-based dataset that has been interpolated to a 1^o latitude x 1^o longitude grid over India and spans each day from 1951–2003. Rajeevan et al. (2006) used rainfall records from 1803 of 6329 available stations that had a minimum of 90% data availability during the entire timeframe so that inconsistencies due to changing station density could be avoided. These stations are highly clustered in western India and become sparser over the northern plains and eastern central India (Figure 2-1). The data were interpolated to a rectangular grid (35 x 32) using a weighted-sum method with radii of influence developed by Shepard (1968).The grid covers the entire country and surrounding waters, but has values of rainfall only over land.

The rainfall data are highly reliable, as the IMD maintains high standards when monitoring precipitation because of its inherent and important role in agriculture (Sikka 2003). Various quality control checks include station location and coding verification, and these ensure that the dataset is a trustworthy one for this study. Rajeevan et al. (2006) compared the IMD gridded dataset with the Variability Analysis of Surface Climate Observations (VASClimo) dataset and found significant correlation between the two. The VASClimo dataset is a new station-based, global-gridded rainfall dataset developed by Beck et al. (2005) that has undergone extensive quality control, thorough interpolation, and error checks between station values and the interpolated values. The two datasets differ only slightly throughout most of India, and correlations exceed 0.8 over Central India. Both datasets also display similar coefficients of variation, and thus, similar trends in interannual variation in rainfall, which is important to this study (Rajeevan et al. 2006).

2.2 Reanalysis

This study uses three different reanalysis products to provide input parameters for use in the back-trajectory program described below. These include the the National Centers for Environmental Prediction/Department (NCEP/DOE) Reanalysis-2 (R2), the NCEP Climate Forecast System Reanalysis (CFSR), and the Modern Era Retrospect-analysis for Research and Applications (MERRA) datasets. From these datasets, we work with surface latent heat flux, surface precipitation rate, surface pressure, specific humidity, temperature, and the u- and v-components of the wind. Potential temperature and precipitable water (PW) are calculated from surface pressure and temperature and from specific humidity, respectively.

First, we use six-hourly global T62 (192 x 81), Gaussian-gridded R2 upper-air (in 17 sigma-pressure coordinates) and land surface data. The data are available from 1979 to the present day. R2 uses the NCEP-based Noah land surface model (LSM), which became operational in 1996. The Noah-LSM predicts land surface water and energy fluxes dynamically and uses a layer-based approach to soil moisture in which governing equations compute the transfer of water within four layers of soil (Kumar et al. 2008). The R2 dataset is considered an improvement over Reanalysis-1(R1) (Kalnay et al. 1996), which had several known processing and human-caused errors (Kanamitsu et al. 2002).

Among the improvements most pertinent to this study (Kanamitsu et al. 2002) is the use of simple rainfall assimilation over land surfaces for better representation of soil moisture. The replacement of model precipitation with an observed 5-day mean (pentad) precipitation from satellite-gauge-based NCEP/Climate Prediction Center (CPC) fixed previous issues where model soil wetness was not reasonably maintained in the tropics (Maurer et al. 2000). Additionally, smoother orography in R2 improved upon the sensible and latent heat fluxes estimated in R1. Several enhancements in model physics led to increases in the accuracy of surface fluxes and land hydrology budgets, and changes in boundary layer parameterizations slightly improved tropical precipitation estimates (Kanamitsu et al. 2002). These changes in parameterizations also improved the estimate of PW or column moisture in R2. The R2 PW more closely approaches the estimates of the National Aeronautics and Space Administration (NASA) water vapor estimates. R2 was intended as an upgrade to R1 (Higgins et al. 2010) and is used in this study as a baseline to compare with our other, newer datasets.

Next, we use six-hourly global T382 (1152 x 576), Gaussian-gridded CFSR upper-air (on 64 pressure levels) and land surface data. The data are available from 1979 to the present day. The dataset also uses the Noah-LSM, which has been updated to include improvements developed since 2005. This dataset was completed in January 2010 and uses a coupled atmosphere-ocean-land surface-sea ice system (Saha et al. 2010).

This dataset is believed to be superior to R2 and R1 because of its model coupling, higher spatial resolution, and more modern data assimilation system (Higgins et al. 2010; Saha et al. 2010). The CFSR atmospheric and land surface models are newer than those for R2, suggesting that CFSR parameters are more current and reliable. CFSR uses satellite radiances instead of the derived temperature or moisture profiles used in R2, which leads to an improvement in the generation of those fields to more closely match observation (Saha et al. 2010). CFSR also uses global precipitation analyses to directly force the land surface analysis. In the tropics, for example, the satellite-based CPC Merged Analysis of Precipitation (CMAP) dataset is highly weighted in the surface analysis. This technique should improve upon the analysis from R2, which relies on "nudging" the soil moisture on the basis of precipitation analysis and prevents this field from deviating far from climatology (Kanamitsu et al. 2002). Higgins et al. (2010) compared CFSR daily precipitation statistics to the CPC Unified Rain Gauge Database and found that they were improved compared to those estimated in R2 and R1. However, according to Saha et al. (2010), the mass balance of the atmospheric water content (given by evaporation minus precipitation) is still "worrisome" in CFSR, as it decreases noticeably after 1998 and could indicate incorrect assimilation of data and potential unreliability of those fields. Thus, the CFSR evaporation estimates should still be treated with caution, as they play a major role in this study.

Finally, we use six-hourly global (540 x 361), Gaussian-gridded MERRA upper-air (on 42 pressure levels) and one-hourly global (540 x 361), Gaussian-gridded MERRA land surface data. The data are a NASA-based product and are available from 1979 to 2007. The dataset uses NASA's Catchment-LSM (CLSM), which, like the Noah-LSM, dynamically predicts land surface water and energy fluxes. However, it uses a topographically based approach instead of a layer-based approach to soil moisture (Kumar et al. 2008). The CLSM uses topographic characteristics and bulk moisture variables to predict soil moisture for each catchment, or computation unit of the model. It then calculates the distribution of moisture at a sub-catchment

level, which is considered an improvement over traditional one-dimension LSMs such as the Noah-LSM. However, Kumar et al. (2008) concluded that both the Noah-LSM and the CLSM exhibit soil moisture that responds similarly to forcing from the atmosphere and yield comparable values for that field.

This dataset is also believed to be an improvement upon the R2 and R1 reanalyses. Like CFSR, MERRA incorporates satellite radiances to fix to the temperature and moisture profile issues possible in the R2 and R1 datasets (Bosilovich et al. 2008). Additionally, MERRA's data assimilation system, the Goddard Earth Observing System-Version 5 (GEOS-5), was shown by Bosilovich et al. (2008) to provide significant improvement over previous NCEP reanalyses regarding precipitation and water and energy cycles. However, Chen and Bosilovich (2008) noted that there is still room for improvement in simulation of the water and energy cycles. This is especially true in tropical latitudes prior to the 21st century, a significant spatial and temporal portion of our study.

2.3 CMORPH

We also incorporate the satellite-based Climate Prediction Center (CPC) morphing method (CMORPH) precipitation estimates (Joyce et al. 2004). These are global precipitation analyses that are available on a high-resolution (eight square kilometer) grid. They are derived from passive satellite microwave scans as well as geostationary satellite infrared (IR) scans. The morphing technique uses motion vectors derived half-hourly from the IR data to advect the precipitation estimates received from the passive microwave data. This technique has been demonstrated to estimate precipitation better than microwave estimates or blended microwave-IR estimates alone.

CMORPH is used to correct the diurnal cycle of precipitation in the different reanalyses at tropical latitudes. It is also used to give our daily IMD rainfall data a diurnal signal, which is required by the temporal resolution of our back trajectory program. The correction technique is described in detail by Dirmeyer and Brubaker (2007). It was used to compensate for known errors in reanalysis precipitation estimates over the tropics, where precipitation is largely convectively driven and encounters problems due to convective parameterization schemes.

2.4 Problems with reanalysis estimates

Finally, it should be noted that model-based estimates, such as surface evaporation rate or latent heat flux, should be viewed with caution. Evaporation is "amongst the most poorly measured hydroclimate fields" (Nigam and Ruiz-Barradas 2006), but it plays an important role in the water balance and evaporative sources of the Earth system as explained above. Since it cannot be directly measured, evaporation is estimated, sometimes inaccurately, from reanalysis land surface models that are driven by observed parameters such as precipitation and temperature (Ruiz-Barradas and Nigam 2004).

Koster el al. (2004) describes that sparse observations of soil moisture and subsequent evaporation prevents a clear demonstration of its impacts on precipitation. They state that these impacts are often seen in atmospheric generation circulation models (AGCMs). Furthermore, Trenberth and Guillemot (1998) concluded that "substantial biases" exist in the moisture fields of the R2 and R1 reanalyses, where tropical structures are not well-defined. We recall studies by Dirmeyer (1999), Arpe et al. (1998), and another by Beljaars et al. (1996) that elucidated the importance of evaporation in modeling. Beljaars et al. (1996) completed a parallel study of two precipitation forecasts with different land surface schemes: one with constrained boundary conditions for soil moisture and another that produced its own soil moisture with input from the atmospheric model. The second scheme resulted in precipitation forecasts that were more realistic, since more moisture was available for evaporation and subsequent precipitation.

Thus, evaporation from land surfaces largely impacts precipitation estimates but is highly dependent on the land surface model used in a given reanalysis. The land surface models have a high potential to be unreliable because of poor model physics, varied resolution, or sparse observations. Since each of the three reanalyses we use in this study has its own land surface model, it is clear that the evaporation parameter will have a prominent effect on the moisture sources we wish to track.

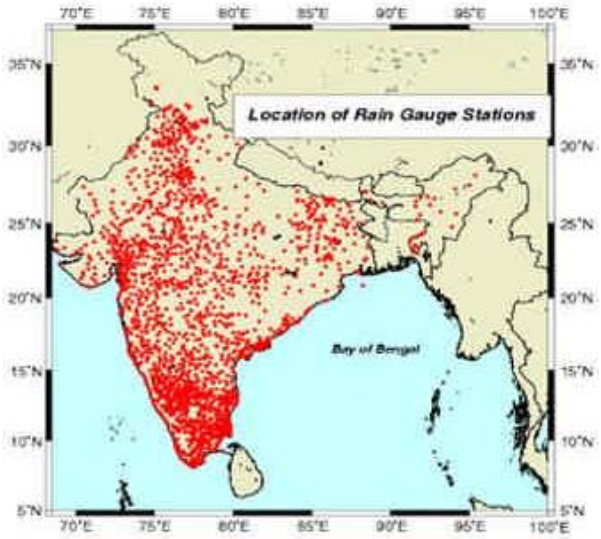

Figure 2-1. The location of rain-gauge stations from which the India gridded rainfall dataset was created. Notice the concentration of stations along west central India and the southern tier and relative sparseness in the west. From Rajeevan et al. (2006).

CHAPTER THREE
METHODOLOGY

3.1 Isolating interannual variability

Rainfall data from the IMD gridded dataset are area-averaged over all-India from June 1 to September 30 for each year from 1951 to 2003. The June-July-August-September (JJAS) period is generally regarded as the peak of the monsoon season, so these months were used to represent the bulk of the rainfall. A climatological area-average rainfall for India was found, and then each year's anomalous rainfall was calculated. The five wettest, driest, and most-neutral years after 1979 were selected and labeled as wet, dry, and neutral years, respectively (Figure 3-1). The years are listed in Table 3-1 below, along with that year's seasonal rainfall deviation from long-term mean rainfall.

Comparison of the results with the central India (73^{o}E-86^{o}E, 16^{o}N-26^{o}N) area-averaged rainfall yielded nearly the same years for each case. Central India is unique to the northern plains and western coast of India in that intraseasonal rainfall anomalies tend to be of opposite sign in this region compared to the others, as described above. Although the results of all-India and Central India interannual variability yielded similar results, we used the all-India wet, dry, and neutral years to capture the annual variability of the entire subcontinent. Rainfall over all-India tends to be highly correlated with rainfall that falls in the "monsoon zone," an area described by Gadgil (2003) that receives significant monsoon rainfall and is "commonly used" in studies of Indian monsoon variability (Lawrence and Webster 2001).

3.2 Isolating intraseasonal variability

Rainfall anomaly data from the IMD were area-averaged over central India for each day (15 May to 15 October) for each of our years of interest. The 15-day "tails" on either side of the monsoon season are important when filtering the data, as explained below, and create a 152 day time series. We defined an intraseasonal, or a single active (break), period to consist of above (below) average rainfall for a period of 10 to 30 days. Thus, an intraseasonal oscillation occurs in the 20-

to-60 day timeframe. We chose to isolate rainfall variations since active and break periods are "traditionally defined" using precipitation factors (Goswami and Mohan 2001), although other studies isolate intraseasonal changes in OLR, winds, or other parameters. Central India precipitation also responds differently than northern or southern India precipitation intraseasonally, so we limited our domain to a box from 73^{o}E – 86 ^{o}E and 16 ^{o}N – 26 ^{o}N.

We then extract the low-frequency 20-60-day mode from the time series using a simple recursive first-order butterworth filter to isolate nonperiodic oscillations of that length (Krishnamurti et al. 1995). The tails allowed us to observe oscillations during the monsoon season without skewing during the JJAS season because of the presence of endpoints. A method similar to this was used by Herndon et al. (1999) [from Lawrence], who used a wavenumber-frequency filter to isolate OLR data over India with periods of 25 to 80 days.

Next, we recorded an active (break) period if a continuous string of 10-30 days was above (below) zero (Figure 3-2). We converted each period's beginning and ending day to pentads, where at least 3 out of the 5 pentad days had to lie in the given period to be assigned to that period. The specific starting and ending dates for each defined active and break period are given in Tables A-1 and A-2, respectively. We used the pentad-to-date conversion (Table A-3) to convert those dates into pentad dates for use in our QIBT.

We compared the intraseasonal oscillations isolated from the butterworth filter and incorporated into our analysis to the actual IMD gridded rainfall data (not shown). For most years, the general trends in increasing and decreasing rainfall throughout the season are well-captured by the filtered oscillations. The actual rainfall data naturally feature more noise that then filtered data. Using the latter allowed us to run our QIBT for more consistent stretches of time than would have otherwise been possible.

3.3 Quasi-isentropic back trajectory program

We use a quasi-isentropic back trajectory (QIBT) program to locate the evaporative sources of precipitation events over central India. Dirmeyer and Brubaker (1999) developed this method for a similar study of evaporative source variability over the central United States. We give a basic description of the program's mechanisms in the following section.

Following the technique of Dirmeyer and Brubaker (1999), we first release one hundred saturated air parcels at every grid point where and when rain has fallen over central India (73^{o}E –

86 ^{o}E and 16 ^{o}N – 26 ^{o}N) at a rate proportional to the precipitation rate at the point. The moisture content of the parcels is equal to the amount of rainfall at the initial grid point. These parcels are assigned a random vertical level that is weighted by humidity so that most parcels are released near the surface, where water vapor is higher. Each parcel is tagged with the environmental potential temperature (calculated from surface pressure and temperature) and isentropically advected backward in time with reanalysis winds. The parcel trajectory is the average of two other trajectories described by Merrill (1989):

1. A backward trajectory locates a parcel from its original point (x^n, y^n) at time *n* to a new point (x^{n-1*}, y^{n-1*}) at time *n-1** using the winds at time *n*.
2. A forward trajectory locates a parcel from point (x^{n-1*}, y^{n-1*}) to another point (x^{n*},y^{n*}) back to time *n* using the winds at time *n-1*.

The backward trajectory and the negative forward trajectory are averaged to arrive at the final point (x^{n-1}, y^{n-1}), which is then bilinearly-interpolated to the nearest grid point. The parcel potential temperature is reevaluated and the parcel is assigned a level in the vertical corresponding to the grid point profile of potential temperature. If the potential temperature of the parcel is found to be lower than the surface potential temperature, it is assigned that value such that the parcel never intersects the ground.

At every time step, we assume that some of the water vapor in the parcel, *k*, comes from the evaporation (*E*) occurring the grid point (*x*,*y*) directly below it. The initial value of parcel moisture level is given by the parcel's fractional contribution to rainfall over initial grid point, *i*, under the assumption that parcels released closer to the surface will contain more moisture than those released at the top of the atmosphere. We then remove water vapor from the parcel at a rate given by:

$$S_{x,y,k,p}(i,j,t) = \frac{E\ (x,y,t)}{PW\ (x,y,t)},$$

where $S_{x,y,k,p}(i,j,t)$ represents the source of moisture for grid point (*i*, *j*) at time *t* contributed by evaporation from remote point (*x*,*y*) into parcel *k* at tracing time *p*. The back tracing continues for a period of 15 days or until the parcel has lost 90% of its moisture because of the moisture removal dictated by $S_{x,y,k,p}(i,j,t)$. Over 95% of these parcels are accounted for by the QIBT after 15 days. We chose to trace the parcels up to 15 days prior to release to conserve moisture for the individual precipitation events. Although atmospheric predictability becomes chaotic after several days (Shukla et al. 1998), we observe that the general spatial layout of evaporative source

is established in five (Figure 3-3a) days and especially ten (Figures 3-3b) days. Extending the sources back 15 or 20 days (Figure 3-3 c–d) does not introduce new sources of evaporation but simply enhances their magnitude. Additionally, the ratio $S_{x,y,k,p}(i,j,t)$ usually has values of 1/10 day^{-1} over most of India since evaporation is an order of magnitude lower than precipitable water values. Thus, we need to trace back longer in time than just ten days to ensure that we have conserved moisture in our parcels. Chan and Misra (2009) and Dirmeyer et al. (1999) follow the same line of reasoning in their studies of back trajectory analysis.

We can predict the character of the evaporative sources on the basis of the reanalysis parameters alone. The rate of removal fraction in the QIBT indicates that remote evaporation and precipitable water values as well as local rainfall values will have large implications on the length of the back trajectories. High evaporation rates and low values of precipitable water lead to a large rate of removal of moisture from the parcels, which will remain localized and fail to trace as far back as parcels passing through environments with low evaporation and high precipitable water. Likewise, at initial grid points where rainfall values are high, the parcels have the potential to trace farther back in time because they contain more moisture that must originate from the environment. Furthermore, reanalysis winds largely dictate the spatial patterns of the trajectories, as they are the source of advection back in time.

We record the evaporative source of the released parcels every pentad (five-day mean) throughout the summer or for specific pentads, depending on the source we wish to isolate. We use pentad-averaged evaporative sources because they are computationally less expensive and because our time scales of interest are larger than five days and are not affected by the time averaging. To calculate total evaporative source for rainfall at a given grid point (i,j) at pentad time t, we take the sum of individual $S_{x,y,k,p}(i,j,t)$ fields from all global grid points (x,y), from all parcels, k, and from the time of the longest trajectory, $p_{f,}$ to get the contribution of evaporation (E) to rainfall over grid point (i,j) in central India:

$$E(i,j,t) = \sum_{x,y} \sum_{k=1}^{m} \sum_{p=0}^{pf} S_{x,y,k,p}(i,j,t)$$

We understand that the area and time sum of these evaporative contributions from all remote grid points over the entire season should nearly equal, but never exceed, the amount of precipitation (P) that fell into the central India domain over the same portion of time.

$$\sum_{i,j,t} E(i,j,t) = \sum_{i,j,t} P(i,j,t)$$

It should be noted that there are potential problems with the technique outlined above. Dirmeyer and Brubaker (1999) showed that there are no precipitation sinks incorporated into the trajectory so that parcel potential temperature is maintained throughout the tracking period. Thus, the only source of moisture is evaporation and the only sink is precipitation, and the possibility of phase changes is not considered. Chan and Misra (2009) suggested that this assumption will overextend the trajectories.

To prepare the reanalysis data for use in the QIBT program, we convert the upper air data from pressure coordinates to isentropic, sigma coordinates so that the parcels follow lines of constant potential temperature. The R2 data were downloaded in sigma coordinates originally, but we manually convert the CFSR and MERRA upper air datasets. To accomplish this task, we run each upper air dataset through a program called p2sig (Documentation), which converts pressure-leveled GRIB data to sigma-leveled spectral coefficients data. We force each dataset to match the 17 vertical sigma levels of the R2 reanalysis, while simultaneously regridding the data to the R2 T62 grid for consistency. We also regrid the CFSR and MERRA flux datasets, as well as the IMD gridded rainfall dataset, to the T62 grid before running the QIBT program so that comparison among the datasets is possible.

3.4 Checking the evaporative source

To check the accuracy of the QIBT program, we compared the program's account of moisture traced back from central India ($\sum_{i,j,t} E(i,j,t)$) with the actual IMD rainfall data, regridded to the T62 grid for comparison. We found the standard error between the estimated moisture originating from evaporative source across the domain and the actual IMD rainfall data and compared the results among the three datasets. We observe that MERRA performed the best in terms of accounting for moisture that contributed to precipitation over central India. MERRA showed a 3.7% error, whereas R2 showed 7.6%, and CFSR showed 10.6% (Table 3-2).

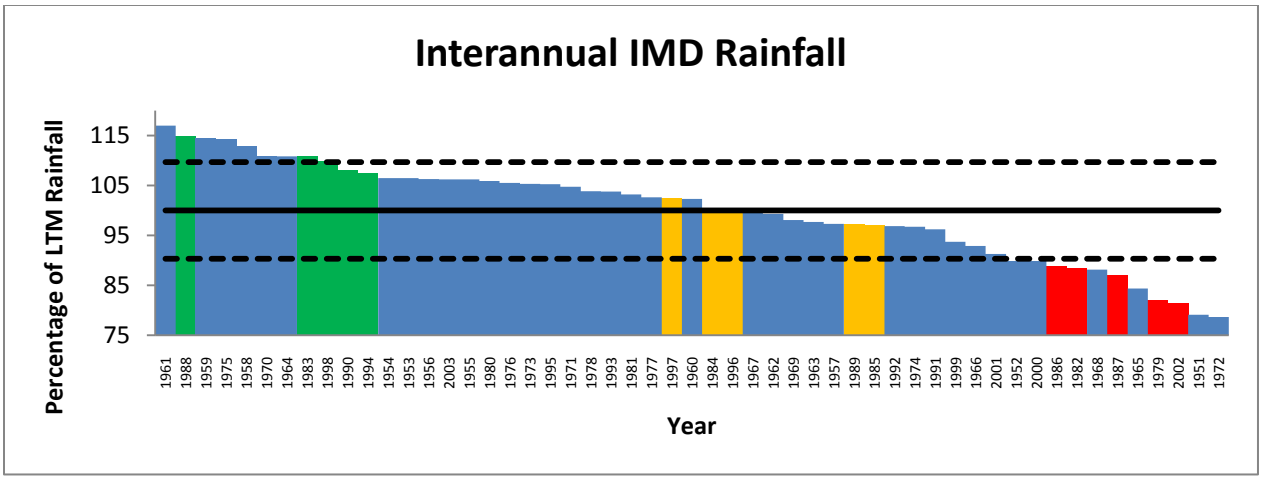

Figure 3-1. Graph showing each year's deviation from climatological (1951-2003) average of seasonal (JJAS) rainfall over all-India. The abscissa is the year (note: not sequential) and the ordinate is the percentage difference between a given year's rainfall and the climatological average. Dry years are colored in red, neutral in yellow, and wet in green. The long-term mean is shown by the black solid line and one standard deviation by dashed lines.

Table 3-1. Specific years chosen (between 1979 and 2003) for wet, dry, and neutral years. The average of all three cases makes up a set of 15 years, which we refer to as "all years," or climatology, for the purposes of this study. Also shown is each year's percentage deviation from the long-term, 53-year average.

Year Cases Selected from IMD Gridded Rainfall					
Wet Years	% of Normal	**Dry Years**	% of Normal	**Neutral Years**	% of Normal
1988	14.9	**2002**	-18.5	**1996**	-0.0
1983	10.8	**1979**	-17.9	**1984**	-0.4
1998	9.9	**1987**	-12.9	**1997**	-2.5
1990	8.1	**1982**	-11.5	**1989**	2.9
1994	7.4	**1986**	-11.3	**1985**	3.0

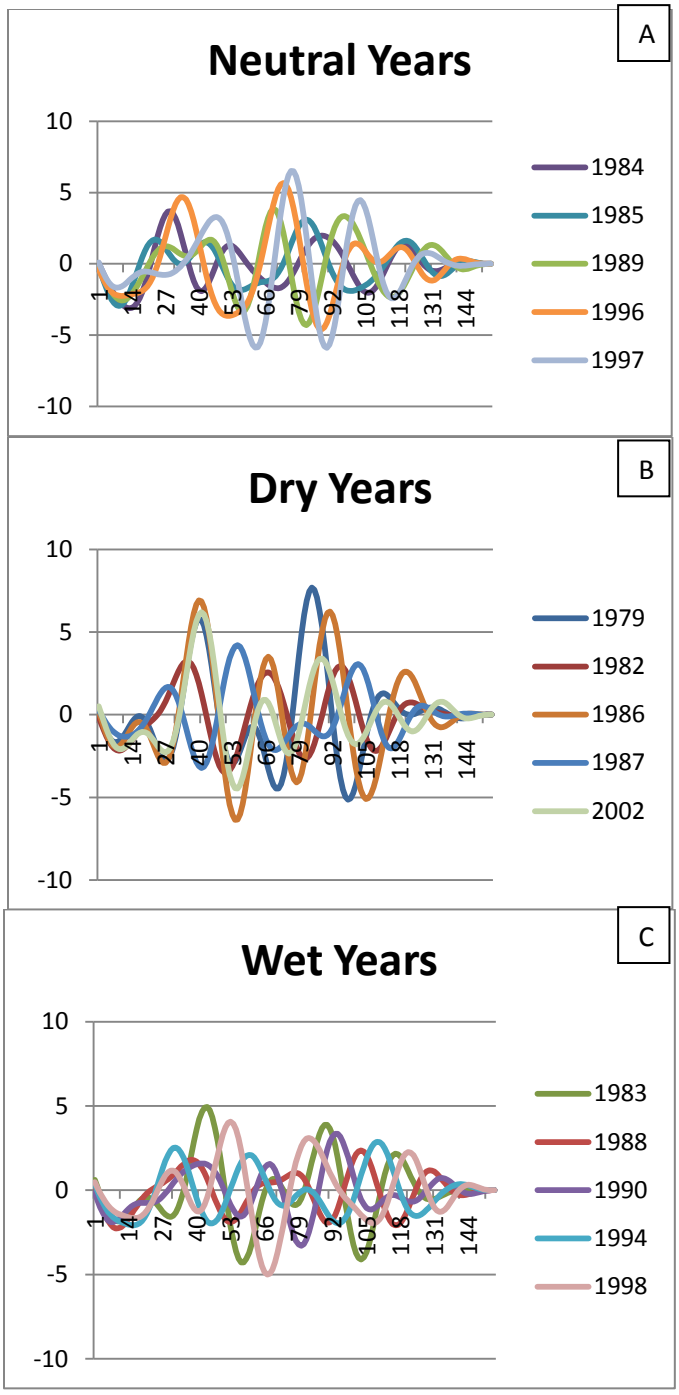

Figure 3-2. Graphs showing the intraseasonal oscillations isolated from the central India area-averaged rainfall data in all (a), dry (b), and wet (c) years. Plots show the rainfall anomalies compared to the yearly average in mm day^{-1}. The abscissa is the season day, starting with 15 May, and the ordinate is the rainfall anomaly in mm day^{-1}. The results have been filtered through a 20-60-day simple first-order recursive butterworth filter.

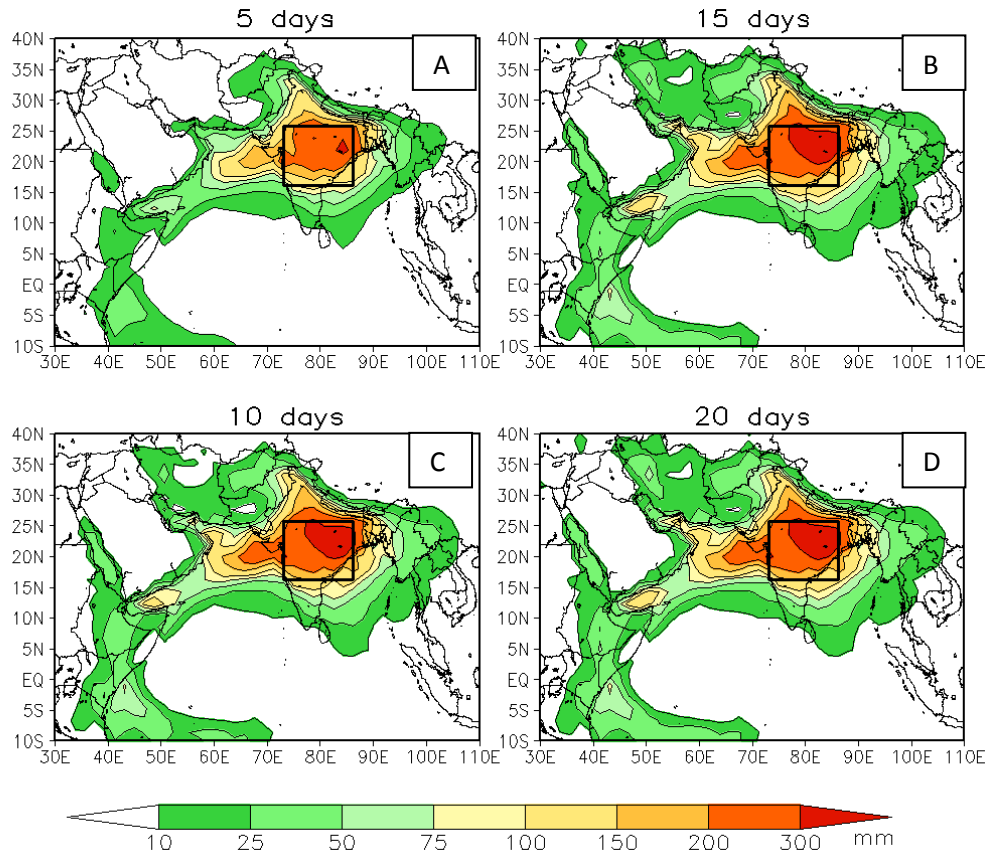

Figure 3-3. Six-hourly average evaporative source for the 1996 (neutral) monsoon season, using parcels traced back for five (a), ten (b), 15 (c), and 20 (d) days. The box represents the central India domain from which parcels were released.

Table 3-2. Percent error between moisture accounted for by the QIBT for rainfall events over central India (seasonal) and the actual IMD rainfall that fell into central India over the same time.

Percent Error between QIBT Estimates and IMD Rainfall		
R2	**CFSR**	**MERRA**
7.6	10.5	3.7

CHAPTER FOUR
RESULTS

4.1 Dataset parameter variability

Our QIBT program uses several surface and upper air variables from each of our three datasets. The variables of most interest to this study are latent heat flux (LHF), low-level (850-mb) winds, and precipitable water (PW). LHF or evaporation and PW are related to the rate of removal of moisture from each of our parcels, whereas the winds act to advect our parcels backward and forward in time (Section 2.3). We first analyze each parameter on a monsoon-seasonal (JJAS) time scale. We then isolate the differences between them on interannual and intraseasonal time scales to identify possible mechanisms to explain the changes in evaporative sources for different rainfall events in different datasets.

We recall initial statements made in Chapter 1 that soil moisture and evaporation dictate rainfall and can influence climate and weather patterns. In the following section, we assume that environmental differences on certain time scales influence our evaporative sources; however, it is likely that character of evaporative sources and weather patterns can influence the environment as well, and it is ultimate difficult to predict cause-and-effect relationships in for these cases.

4.1.1 Seasonal average

As described previously, model-based evaporation estimates are among the most important (but most difficult to estimate) parameters used in this study. Thus, we expect any changes in evaporation estimates to manifest themselves as changes in the magnitude or position of evaporative sources for our rainfall events especially over land, where moisture is limited. LHF is directly related to evaporation by accounting for the latent heat of vaporization, and it is used to represent each model's estimated evaporation field. We see that R2 six-hourly average seasonal evaporation is highest over the tropical Indian Ocean with maxima over the southern Bay of Bengal and southwestern Arabian Sea to the north (Figure 4-1a). Both regions exhibit evaporation of over 6 mm day^{-1}. As expected, evaporation is low over the desert regions and the

Tibetan plateau north of India, where moisture and evaporation are limited. Evaporation is moderate (2 mm day^{-1} – 4 mm day^{-1}) over the Indian subcontinent, where it decreases in magnitude from the south to the north. Evaporation is also increased around smaller water bodies in the domain such as the Persian Gulf and the Red Sea, where moisture is less limited than in surrounding land regions.

When compared to CFSR (Figure 4-1b), R2 exhibits significantly greater evaporation over eastern central India (10% – 25% increase), northern India (over 100% increase), and also over the southern tip of the subcontinent (over 100% increase). Over much of the eastern Arabian Sea, R2 shows significantly less (10%–25%) evaporation compared to CFSR. Overall, R2 estimates greater evaporation over land and less evaporation over water when compared to CFSR, despite the fact that each incorporates the same Noah-LSM. MERRA shows significantly more evaporation over northwestern India (over 100% increase) and over the tropical Indian Ocean and Bay of Bengal (10% – 25% increase) when compared to R2 (Figure 4-1c). Small areas of significant reduction in LHF in R2 are observed over far western central India (up to 50% reduction) in this comparison. The differences between the newer datasets could be attributed to their use of different LSMs.

We consider the seasonal six-hourly average diurnal cycle of evaporation estimates for each dataset to check for consistency (Figure 4-2). All reanalyses show similar magnitude peaks in evaporation of around 7 mm day^{-1} – 8 mm day^{-1} of evaporation around 06Z over central India. R2 (MERRA) exhibits more evaporation compared to the other datasets prior to (after) 06Z. Overall, CFSR exhibits the lowest rate of evaporation among the datasets throughout the day, whereas R2 features the most. This result helps to explain why CFSR had the greatest standard error when comparing moisture contained in evaporative sources to total rainfall (Section 3.4). Low evaporation over land forces the parcels to trace further back in time in CFSR, which leads to less conservation of moisture in that dataset.

We also isolate six-hourly average seasonal 850 mb winds to confirm the presence of the low-level cross-equatorial flow passing north over the eastern coast of Africa, across the Arabian Sea, west over the Indian region, and exiting the domain through southeast Asia. In R2 (Figure 4-3a), this feature is well noted, with winds in excess of 20 ms^{-1} throughout most of cross-equatorial flow region. Differences in the low-level winds between R2 and MERRA are small (less than 5 ms^{-1}) and directionally varied over this region (Figure 4-3c), and most of the large

anomalies in the field (greater than 5 ms^{-1}) lie over the land portions of southern China and eastern Africa, well away from most monsoon activity. However, differences in the wind between R2 and CFSR are more noticeable (Figure 4-3b). Here we see strong (up to 5 ms-1) easterly anomalies over the southern Arabian Sea and southern Bay of Bengal when comparing R2 to CFSR. These anomalies demonstrate that the cross-equatorial flow in R2 is weaker than the cross-equatorial flow in CFSR.

Next, we analyze six-hourly average seasonal PW values for R2 (Figure 4-4a). As we saw for the evaporation field, PW values are highest over the Bay of Bengal, Southeast Asia, and southeastern India (over 55 mm) and decrease across the subcontinent toward the northwest (35 – 50 mm). Values are low over the desert regions and the Tibetan plateau, where the high elevation and subsidence limits atmospheric humidity. CFSR (Figure 4-4b) and MERRA (Figure 4-4c) estimates for PW are significantly higher (up to 25% increase) over eastern central India and the Bay of Bengal compared to the estimates from R2. The values in R2 are also higher than those from the other datasets over most of eastern Africa and the far eastern Indian Ocean. These results suggest that R2 has universally more (less) column moisture over eastern Africa (central India) across our other two datasets. The similarities between CFSR and MERRA suggest more consistent column moisture modeling in these datasets possibly due to their incorporation of satellite radiances, which are not used in R2.

Finally, we consider the six-hourly average seasonal ratio of evaporation to PW ($\frac{E}{PW}$) in each dataset. We used this ratio to fractionally remove moisture from parcels that were released over central India. Parcels that advect back through regions of high (low) $\frac{E}{PW}$ lose moisture quickly (slowly) and will tend to remain local (advect remotely) compared to the case in which parcels advect through a neutral environment. For R2 (Figure 4-5a), we observe that the ratio is around 10% over much of India, and that it increases to around 15% over the tropical ocean and the nearby smaller seas where evaporation is increased. The ratio is low over the desert regions where evaporation is almost zero. When compared to CFSR (Figure 4-5b), R2 shows a significant increase (30% – 60%) in the ratio over eastern central India and Southeast Asia. The ratio is significantly lower (10% – 30%) over the eastern Arabian Sea and the southern Bay of Bengal. When compared to MERRA (Figure 4-5c), R2 shows a generally higher ratio over

eastern central India, the Bay of Bengal, and the tropical Indian Ocean (20% – 60% increased), as well as a significantly lower ratio (10% – 30%) over southern China.

Although the moisture removal ratio differs between datasets, we understand that the rate of moisture removal is exponential; that is, parcels with greater moisture content will lose moisture faster than parcels with lower moisture content while advecting backward through the same region. Thus, this ratio explains only part of the difference in evaporation sources that we trace, as several other factors, including the low-level winds and the rainfall patterns, contribute to the positioning and character of each parcel as well. Additionally, the magnitude of the ratio is most important closest to the area of release, where parcels have the potential to lose the most moisture while advecting backward in time.

4.1.2 Interannual variation

We compare the various parameters on an interannual time scale to help explain any potential changes that we isolate in evaporative sources during wet years and dry years. In the six-hourly seasonal average 850 mb wind field, all three datasets show similar differences between wet years and the average and between dry years and the average. During wet monsoon seasons (Figure 4-6a–c), we see an increase in the overall monsoon circulation and the cross-equatorial flow with an enhancement in the westerly winds (~2 m/s) over the Arabian Sea and across the southern tip of India in all datasets. These eventually loop back over the Bay of Bengal and turn southeasterly across eastern central India. In comparing dry years to average (Figure 4-6d–f), we see anomalous easterly winds (~2 m/s) passing over southern India and into the Arabian Sea, with northwesterlies over eastern central India in all datasets. This result suggests an overall weakening of the monsoon flow during dry years and is consistent with results from Krishnamurthy and Shukla (2000).

We also consider the interannual variation of the six-hourly seasonal average $\frac{E}{PW}$ ratio. During wet years, we observe a decrease (2.5% – 10%) in the ratio over parts of the Arabian Sea and the western tropical Indian Ocean in all three datasets (Figure 4-7a–c). Both R2 and CFSR feature a similar decrease (2.5% – 10%) in the ratio over the central Bay of Bengal. This extends over central India in MERRA. This reduction pattern is attributed to the increase in the PW field over most of the cross-equatorial flow region during wet years (not shown). During dry years, we notice an increase (2.5% – 10%) over the Arabian Sea in all datasets (Figure 4-7d–f), but the difference is larger in MERRA than it is for R2 or CFSR. We attribute this pattern to the

decrease in PW available for dry years along the cross-equatorial flow path (not shown). In the case for CFSR, we also observe a small increase over the Bay of Bengal during dry years.

None of these changes in the $\frac{E}{PW}$ ratio in either case is significant, however, so we are uncertain about the contribution of changing environmental moisture to evaporative sources on an interannual time scale. The changes are also remote from central India and therefore have les influence on the parcel tracks than if the changes were closer to the release region. We assume that the change in the wind field at this time scale will dictate the position and magnitude of our evaporative sources.

4.1.3 Intraseasonal variation

We notice consistent changes in the six-hourly intraseasonal average 850 mb wind fields for each of the datasets. In active periods from all datasets (Figure 4-8a–c), we isolate a 4–5 m/s increase in the southwesterly component of the winds over the Arabian Sea and across southern India, similar to what we saw for the composite of wet years, but with a larger southerly component. The winds turn anomalously northward over Southeast Asia and then back toward the northern plains of India as southeasterlies. No particular dataset features a wind pattern unique to the others. Likewise, break periods feature nearly the opposite pattern in anomalous winds (Figure 4-8d–f), which is consistent with results from Krishnamurthy and Shukla (2000). They concluded in their study that active and break periods are associated with an enhancement or reduction in the overall seasonal monsoon circulation. We know that TCs and low pressure systems advect from the Bay of Bengal during active periods, but we cannot resolve their contribution to the wind field at this resolution.

We also observe intraseasonal variation in the six-hourly average $\frac{E}{PW}$ ratio for each dataset. In active periods from all datasets (Figure 4-9a–c), we see a significant increase (up to 12.5%) in the ratio over the Bay of Bengal, particularly in the western edge of the basin. In R2 and CFSR, this increase extends across to the eastern Arabian Sea. In all cases, portions of northern central India feature a non-significant decrease in the ratio (2.5 – 12.5%). During active periods, the precipitable water and especially the evaporation fields increase compared to average (not shown) over these areas, which helps to explain the increase in ratio we observe during these times. During break periods from all datasets (Figure 4-9d–f), we notice the opposite pattern. Areas around the western Bay of Bengal have significant lower-than-average

$\frac{E}{PW}$ ratios, and this reduction extends to the eastern Arabian Sea for CFSR and R2. Portions of northern India also exhibit a non-significant increase in the ratio for all three datasets. Likewise, during break periods, precipitable water and especially evaporation show reductions compared to normal over these areas, which explains the reduction in the ratios that we observe.

We attribute the existence of high moisture potential near the Bay of Bengal during active periods to the presence of LPSs in that area during those periods. Since these changes occur close to central India, we expect them to have a larger impact on the evaporative sources compared to the interannual variation case.

4.2 IMD rainfall variability

IMD gridded rainfall data (Section 2.1) form the core precipitation input for our back trajectory program, so we graphically analyze their interannual and intraseasonal variability over India to confirm that our methodology properly isolated the expected modes of variation.

4.2.1 Interannual variation

We first set out to characterize the daily-average seasonal (JJAS) rainfall patterns over India. In all analyzed years (Figure 4-10a), rainfall maximizes over central India, especially along the southwestern coast and far eastern portion of the country. This result agrees with the climatology discussed extensively in literature (Rajeevan 2003; Gadgil 2003). A majority of our released parcels will originate from these regions. As expected, the composite of wet years features a higher amount of rainfall across the entire subcontinent compared to the climatological average rainfall (Figure 4-10c). Likewise, the composite of dry years features a decrease in magnitude of seasonal rainfall (Figure 4-10b), with the same overall spatial pattern that we see for all years and for wet years.

We also take our composite of wet years and our composite of dry years and compare them to all analyzed years. We notice small (less than 30%) differences in the daily-average rainfall amounts in wet years compared to all years over most of central India (Figure 4-11a). These differences are significant over only the central-most portions of the region. The differences are larger (30 – over 50%) and statistically significant in the far western potions of the country. Likewise, the differences between dry years and all years are small (less than 20% reduction) and not significant over central India (Figure 4-11b). The differences are larger (up to

50%) and significant in the far western portions of the country. This result concurs with previous studies that have found a small standard deviation in the seasonal rainfall compared to the mean, which makes it difficult to study changes in the monsoon rainfall on this time scale and with this sample size. It is interesting to note that most of the significant difference between wet and all years and dry and all years lies outside the central India box. Thus, we would assume any interannual changes in evaporative source to be due to some parameter other than a significant change in rainfall patterns on this time scale (Section 4.1).

4.2.2 Intraseasonal variation

Next, we choose to isolate the daily-average rainfall patterns during the active and break periods of the Indian monsoon. The composite of active periods from all years (Figure 4-12a) looks very similar to the pattern we saw for the wet year composite (Figure 4-10c). Rainfall is maximized over central India and especially over the southwestern coast and far eastern portion of the country. During break periods (Figure 4-12b), the maximum in rainfall shifts further toward the east where more rain occurs over the northern plains and less falls over the central India region.

The largest difference between the active and break periods and average conditions is located mainly along the central and western portions of the subcontinent. In active periods (Figure 4-13a), rainfall is significantly increased (up to 50%) within the western half of the central India box, extending toward the coast of the Arabian Sea. There is some (less than 30%) drying along the northeastern and southern portions of the country. This pattern is nearly opposite to the one we see for break periods (Figure 4-13b). There is significant drying (up to 50%) in the western and central portions of the country, with a slight increase (up to 30%) in rainfall in the northern plains and southern tip of India. This pattern, anomalies of one sign over central India and the opposite sign to the north and south, was described by Krishnamurthy and Shukla (2000) and shows that the methodology used to isolate intraseasonal variation was successful. These results tend to be more statistically significant than those we saw for interannual variability, but we attribute this difference to the increased sample size for and greater variance in intraseasonal periods compared to interannual periods.

Since there is more change in rainfall amounts over central India on this time scale, we expect precipitation amounts to play a larger role in dictating intraseasonal evaporative sources than in dictating interannual evaporative sources. We also observe that most intraseasonal

rainfall change occurs over western central India, so during active (break) periods, more parcels will be released from western (eastern) portions India compared to average.

4.2.3 Interannual variation of intraseasonal events

Finally, we compare our rainfall data to isolate any interannual variability in the intraseasonal oscillations of daily-average rainfall patterns. We find that during wet years, active periods are significantly (10% – 100%) wetter than average over all of central India and most of the western and northern portions of the country (Figure 4-14a). In dry years, however, active periods have anomalies of a mixed sign across India and are not completely "wet" (Figure 4-14b). There is a significant (10% – 50%) increase in rain over central and western India, but a significant (10 – 50%) drying over the northern plains compared to average. Likewise, during dry years, break periods tend to be universally drier (10 – 75%) compared to average (Figure 4-14d), with some significance in eastern central India and in the northernmost parts of the country. In wet years, break periods are actually wetter than the climatological average (Figure 4-14c) and significant increases (10% –100%) in rainfall occur all around the central India region.

Since the rainfall difference patterns between wet and dry years for both active and break periods are not symmetrical about the mean, we assume that there is some interannual signal in the intraseasonal oscillations. We certainly observe this for break periods from wet years, where the seasonal, flooding influence impacts the break periods and makes them wetter than normal. Thus, we expect there to be some interannual change in the evaporative source on this time scale since our parcels will be released over different locations with different rates and moisture quantities depending on the seasonal and intraseasonal character of the monsoon.

4.3 Evaporative source variability

The ultimate goal of this study is to isolate and document changes in the location, extent, and magnitude of the evaporative sources for seasonal and intraseasonal rainfall events during the Indian monsoon.

4.3.1 Average variability

We begin by analyzing the evaporative sources for the six-hourly seasonal (JJAS) average rainfall events during all years for R2 (Figure 4-15a). The evaporative source is largely concentrated over eastern central India, where terrestrial evaporation presumably plays a role in providing moisture for local rainfall events. The sources extend to the east across the Bay of

Bengal and diminish over Southeast Asia. The sources also extend to the west and south across the Arabian Sea, the smaller nearby seas, and toward the eastern African coast and Madagascar. These remote influences could be attributed to large evaporation and high moisture ratio over the water bodies and the African landmass and subsequent advection of that moisture to central India via the cross-equatorial flow. The increased onshore flow off the Bay of Bengal during active periods explains how this moisture could feed into central India from the east, which is located generally downstream of the seasonal cross-equatorial flow. Finally, we see a small extension of high-magnitude evaporative source over northwestern India and northern Pakistan, where evaporation and moisture ratio are locally high and winds are weak. It is possible that moisture from surface evaporation in this region is pulled southward to supply moisture for rainfall events to the southeast.

Identical plots for composites of wet years (Figure 4-15b) and dry years (Figure 4-15c) are also supplied for comparison with the case for all years. Differences on this time scale will be explained in the next subsection. Spatial layout is generally similar among the cases, and the biggest differences are found in the magnitude of the moisture sources.

We have also included identical plots for the evaporative sources isolated from both CFSR (Figure 4-16) and MERRA (Figure 4-17) for consistency and comparison to R2. Overall spatial distribution and magnitude of the evaporative are similar between the three cases, but there are major differences between them in certain regions.

There are significant differences in the six-hourly average evaporative sources between R2 and CFSR. In R2 (Figure 4-18a), we observe a significant increase (25%–125%) in evaporative sources over north-central and northwestern India, where R2 exhibited greater evaporation and moisture ratio compared to CFSR. In this region, parcels would potentially remain more localized in R2 since they could lose moisture more quickly in that environment. When compared to CFSR, R2 shows a significant decrease (25%–75%) in moisture contribution from the Bay of Bengal, the Arabian Sea, Southeast Asia, and eastern Africa. Over the oceanic regions, R2 has lower moisture potential and lower winds (specifically over the Arabian Sea) than does CFSR. Such conditions support lower marine moisture advection in contribution to total rainfall over India. The general lack of remote moisture advection from terrestrial and marine sources in R2 can also be explained by the previously mentioned local increase in moisture recycling over northwest India. It is plausible that this scenario places less demand on

remote sources for moisture since most moisture is originating locally and within the system itself.

When we compare the results of R2 to the results of MERRA (Figure 4-18b), we notice a somewhat similar result. Compared to MERRA, R2 features greater (25%–125%) moisture contribution from northwestern India. This is related to the increase in evaporation and moisture ratio fields in R2 compared to MERRA over the region. Again, evaporation from the north releases more atmospheric moisture into the column in R2 than in CFSR, which could later feed nearby precipitation events. As we saw in the case for R2 and CFSR, there is a reduction (25% – 50%) of remote moisture advection in R2 compared to MERRA. We recall that R2 featured higher evaporation and moisture ratio over the Bay of Bengal compared to MERRA. Thus, parcels advecting back through this region would tend to dry out quickly in R2 compared to MERRA and thereby decrease the influence of more remote regions. However, unlike the case for R2 and CFSR, there is a significant increase (50%–150%) in evaporative source from the far eastern Indian Ocean in R2 compared to MERRA. In this case, local evaporation differences over India are not as large between R2 and MERRA as they are for R2 and CFSR. Therefore, R2 would advect more moisture from remote areas; the eastern Indian Ocean shows increased moisture ratio in R2 compared to MERRA, which could explain the observed contribution of this area to central India moisture.

These results regarding local-to-remote evaporative source influences are confirmed in our analysis of the recycling ratios for each dataset (Table 4-1). In each case, R2 exhibits the highest ratio of local to remote evaporative source. CFSR and MERRA show similar ratios, each of which is lower than that of R2.

4.3.2 Interannual Variation

Next, we choose to isolate differences in the magnitude and location of the six-hourly average evaporative sources in wet years and in dry years. Here, we see patterns that are relatively consistent and expected in each of the datasets.

First, we compare wet years to all years for R2 (Figure 4-19a). We observe a general increase in the evaporative sources from all the regions we observed in Figure 4-15. As expected, moisture contribution is higher from all regions because rainfall is increased in wet years compared to average. This result confirms the proposal that the overall monsoon flow is enhanced in wet years compared to dry (Krishnamurthy and Shukla 2000). However, there are

significant increases (10%–40%) in small portions of the western Arabian Sea and central India in R2. The results are similar for CFSR (Figure 4-19b) and small, significant increases (10%–50%) occur over the eastern Arabian Sea and western central India. For MERRA (Figure 4-19c), small significant increases (10% –50%) occur over the eastern Arabian Sea and central India.

The significant enhancement of moisture sources from these specific regions demonstrates that local evaporation over India and remote advection from marine areas of the cross-equatorial flow region contribute more to the universal increase in moisture source in wet years than do terrestrial regions to the north and remote regions to the east. Although the moisture ratio is decreased across much of the domain in wet years, the changes in the ratio are far located from central India, and they are assumed to have little influence on the moisture content of our advected parcels. Since the winds are increased along the cross-equatorial flow region in wet years, it is possible that more parcels follow that trajectory back in time and that we isolate more moisture contribution from areas to the west as a consequence.

For dry years, we observe an overall decrease in the magnitude of the evaporative sources compared to all years for all datasets. For R2 and MERRA (Figure 4-19 d;f), the evaporative source is significantly reduced (10%–50%) over northwestern India; for CFSR (Figure 4-19e), the source is significantly reduced (10% to over 50%) over the Arabian Sea. The case for dry years is somewhat different than the case for wet years. For dry years, only CFSR shows that most of the universal reduction in moisture occurs over the cross-equatorial flow region where low-level winds are anomalously weaker compared to average. This case is opposite to the one observed for wet years. However, for R2 and MERRA, most of the reduction occurs more locally and could be influenced more by changes in moisture availability in those areas and less by the overall flow, which is weaker than average in dry years and would have less influence in the back trajectories.

Overall, the mechanisms governing wet year and dry year moisture regimes over central India are on a large scale and involve changes in the increase or reduction of mostly remote moisture influence for rainfall events. The TBO and Eurasian snow cover mechanisms are two such phenomenons that occur along with an interannual increase or decrease in overall monsoon flow and could explain the changes we observe here. However, it has been shown that moisture sources become enhanced (reduced) over different regions of the overall monsoon flow during

wet (dry) years. This finding suggests that interannual moisture variability involves more than a simple oscillation of the overall flow about the climatological mean as this study has assumed.

4.3.3 Intraseasonal variation

We now observe the differences in location and strength of the six-hourly average evaporative sources for active and break rainfall events during the Indian monsoon. For both R2 (Figure 4-20a) and CFSR (Figure 4-20b), we see that active periods feature a significant increase (up to 50%) in evaporative source over the northeastern Bay of Bengal, which extends westward over the Arabian Sea but is not statistically significant. This result is seen in MERRA as well (Figure 4-20c), but the difference is significant in the Arabian Sea and central India.

Over the Bay of Bengal, we recall that the moisture ratio is significantly increased in active periods compared to average, suggesting higher potential of moisture gain or loss over this region. Therefore, any parcels advecting back over the bay will tend to dry out quickly and remain more localized over that region than they would while passing through a neutral environment. The increase in southeasterly component of the wind during the active periods also forces our parcels to take trajectories that pass through this region more so than they would based on climatology. We suggest that these changes could alter our evaporative sources, and we attribute the changes to enhancement in overall flow of the monsoon as well as the presence of LPSs and TCs that move over India from the Bay of Bengal (Chapter 1.3). In this scenario, TCs act as major sources of moisture, which, along with the enhancement in background flow, could explain why the Bay of Bengal contributes more moisture to central Indian rainfall events during active periods. The increase in moisture contribution from the Arabian Sea in MERRA suggests that both the cross-equatorial flow and TC activity could be contributing to the overall enhancement in moisture over India that we observe during active periods.

We see a cross-correspondence with the results for all break periods (Figure 4-20d–f). In this case, there is a decrease in evaporative source overall most of the domain (up to 50%) and most significance lies over the northeastern Bay of Bengal. One exception is the evaporative source isolated from MERRA (Figure 4-20), which features significant reductions westward into the Arabian Sea. We attribute these changes to the absence of the mechanisms we previously suggested for the active case. In this case, TCs and LPSs are absent and the overall monsoon circulation is weakened compared to active periods, so the largest reduction in moisture

contribution occurs over the Bay of Bengal where moisture heavily originates during the active periods.

Finally, we note that the largest change in rainfall during active periods occurs over western India, and only MERRA suggests that local evaporation and moisture recycling over central India may play a role in contributing to or reducing moisture at this time scale.

4.3.4 Interannual variation of intraseasonal events

The topic of most interest to this study is the interannual variability of intraseasonal oscillations in central India rainfall. We have previously considered the possibility of interannual variation of the ISOs, but we have not quantified this phenomenon. We now attempt to isolate it in the location and strength of the six-hourly average evaporative source.

For R2, we see a distinct interannual signal in the intraseasonal oscillations. First, we compare all active periods from wet years (Figure 4-21a) to all active periods from dry years (Figure 4-21c). There is a significant increase (75% – 100%) in the evaporative source over the northeastern Bay of Bengal and a small significant increase (50% – 75%) over central India and the far eastern Arabian Sea. In this case, we assume that both the interannual, increased circulation mechanism, as well as the intraseasonal, TC mechanism, are playing a role in characterizing the evaporative sources. When we look at all active periods from dry years, however, we see a different pattern. There is a slight reduction in evaporative source remotely over the northern Arabian Sea and locally over northern India but no areas of significance. We do not observe an increase in moisture from the Bay of Bengal as we saw for all active periods, but we do see some reductions collocated along the same regions where we isolated reductions in evaporative source during dry years. Thus, moisture sources are favored in different regions during a given intraseasonal oscillation depending on the interannual signal that occurs along with it. This gives credence to arguments that there is an interannual signal in the intraseasonal oscillations of the monsoon.

Likewise, for break periods, we observe cross-correspondence in the evaporative source patterns. Break periods from wet years are, in fact, associated with increased contribution of moisture from remote regions and a lack of moisture contribution from the Bay of Bengal (Figure 4-21b). This suggests the influence of both interannual and intraseasonal moisture source patterns that we isolated earlier. When we isolate the evaporative source of break periods from dry years (Figure 4-21d), we see reductions in the same general areas where we saw increases for

active periods from wet years. Only the region over the far northeastern Bay of Bengal features a significant reduction (over 50%) in the evaporative sources. Again, we assume that during break periods from dry years, the contribution of moisture from the Bay of Bengal and the cross-equatorial flow regions reduces, leading to the reduction in evaporative sources that we observe. We conclude here, too, that is important to note the interannual signal when considering the break phase of the intraseasonal oscillations.

Interestingly, these results are consistent among our three datasets. We consider the same plots for CFSR (Figure 4-22). For all active periods from wet years, we see that the evaporative source is enhanced in nearly the same location as it is for R2. The same is true for all active periods from dry years, all break periods from wet years, and all break periods from dry years, with significant reductions (over 50%) over the Bay of Bengal and the Arabian Sea in the last case, where dry years feature significant reductions in moisture over the same areas. For MERRA (Figure 4-23), the spatial patterns of the evaporative sources in each of these cases are nearly identical to those of R2 and CFSR. For MERRA, we observe greater significance in both the wet active and the dry break cases that we do for either R2 or CFSR, as well as a significant reduction (25% – 50%) over northwestern India in dry active periods. We recall large areas of significant enhancement or reduction in moisture source for MERRA at the intraseasonal time scale, as well as a reduction of moisture from northwestern India during dry years. Again, since we observe the effects of large scale and local changes in moisture sources, we assume that both interannual and intraseasonal mechanisms are governing the sources of moisture for these individual events.

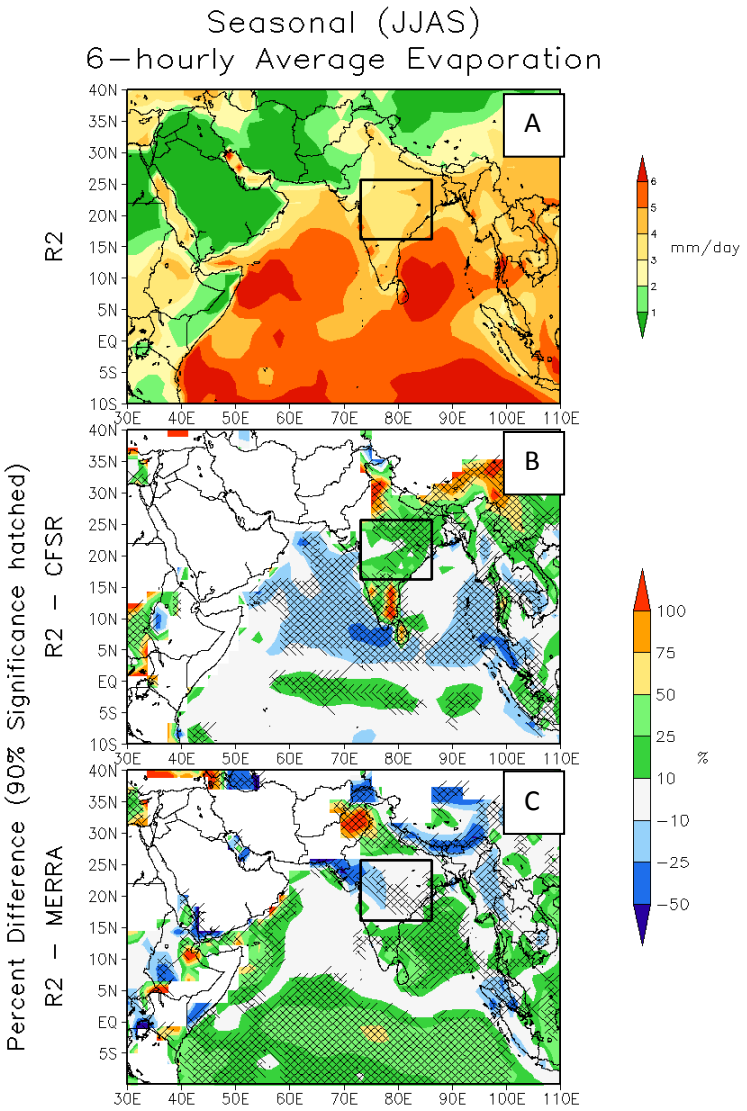

Figure 4-1. Six-hourly average evaporation rate (mm day^{-1}) for the monsoon season (JJAS) for R2 (a), and the percentage difference between R2 and CFSR (b) and R2 and MERRA (c). The percentage difference is given by the difference between the first field and the second field divided by the second field so that when comparing R2 – CFSR, the percentage refers to "number of times greater than CFSR." This technique is widely used in this study and is the same for each plot that features it. Areas that are 90% significant, according to a two-tailed t-test, are hatched. Regions of small evaporation (< 1 mm day^{-1}) are masked out so that the percentage difference over the desert regions does not reveal extremely large values due to division by small numbers. The square box represents the region from which we released our parcels and is the same for every subsequent figure.

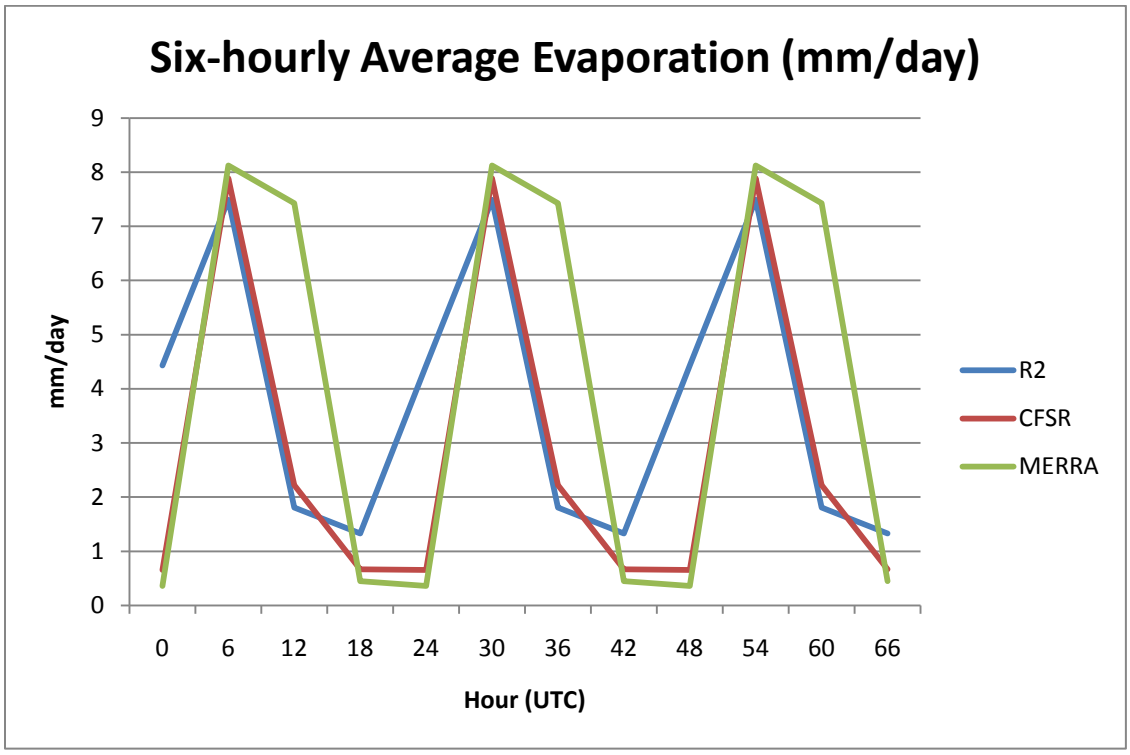

Figure 4-2. Diurnal cycle of six-hourly average evaporation for each dataset over central India. Three cycles are shown to demonstrate the oscillation from day to day. The abscissa is the time step in UTC time, and the ordinate is evaporation in mm day^{-1}.

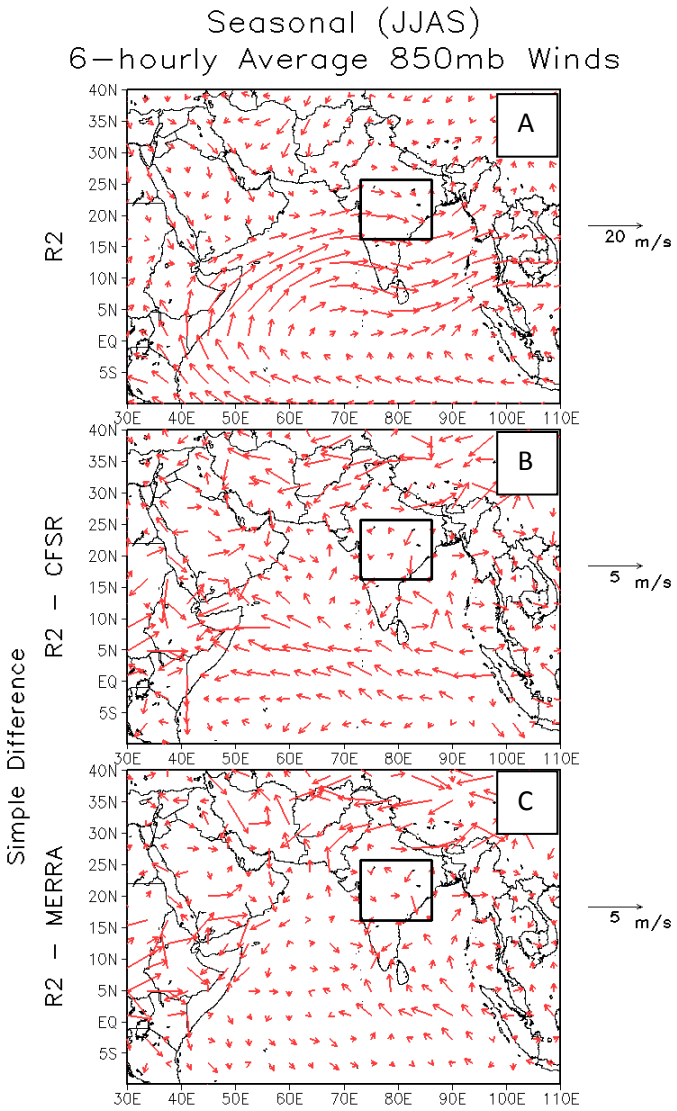

Figure 4-3. Same as Figure 4-1, but for six-hourly average 850 mb winds. Scale is shown to the right of each subplot (note difference between (a) and (b) and (c)) and areas of significance are not hatched here. No mask is used as this is a simple difference between the fields.

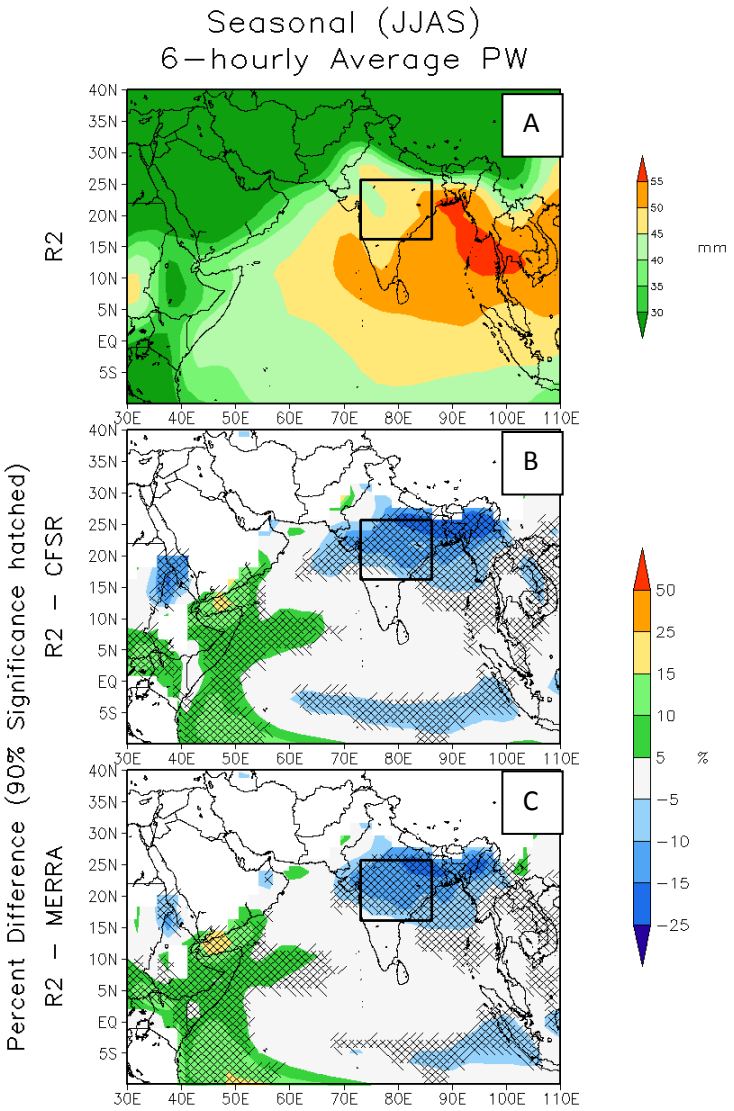

Figure 4-4. Same as Figure 4-1, but for six-hourly average PW. PW was calculated by taking the vertical integral of the specific humidity field up to 275 mb in GrADS. Areas of low PW (< 5 mm) are masked out.

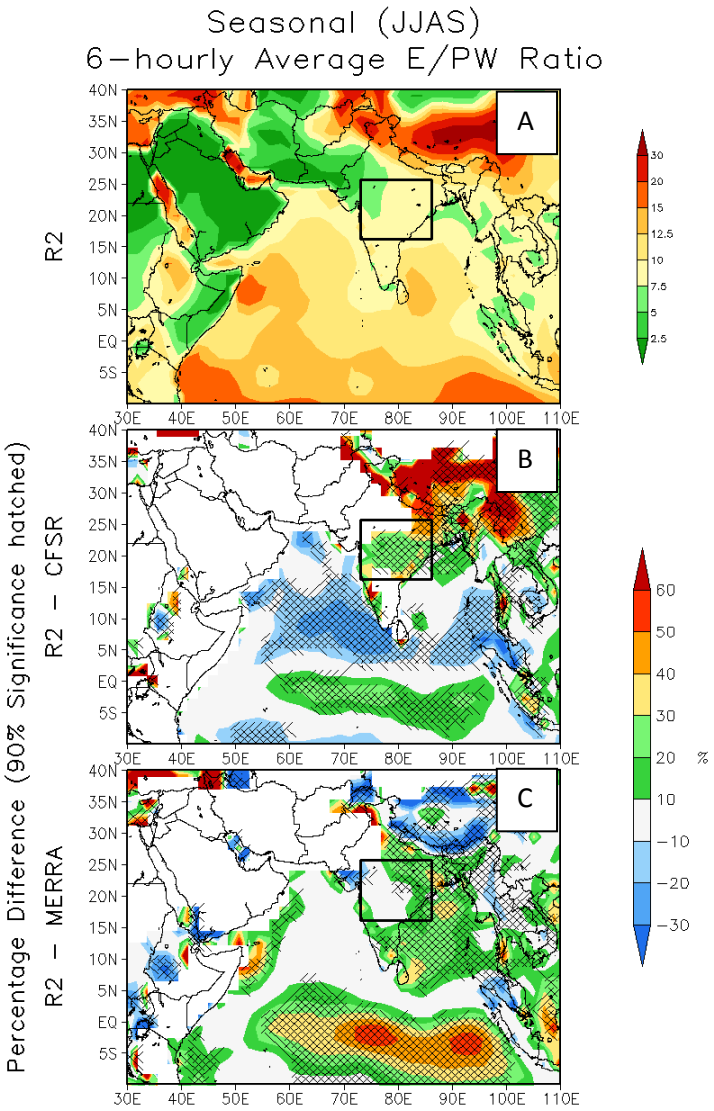

Figure 4-5. Same as Figure 4-1, but for six-hourly average $\frac{E}{PW}$ ratio. Areas of low ratio (< 5%) are masked out.

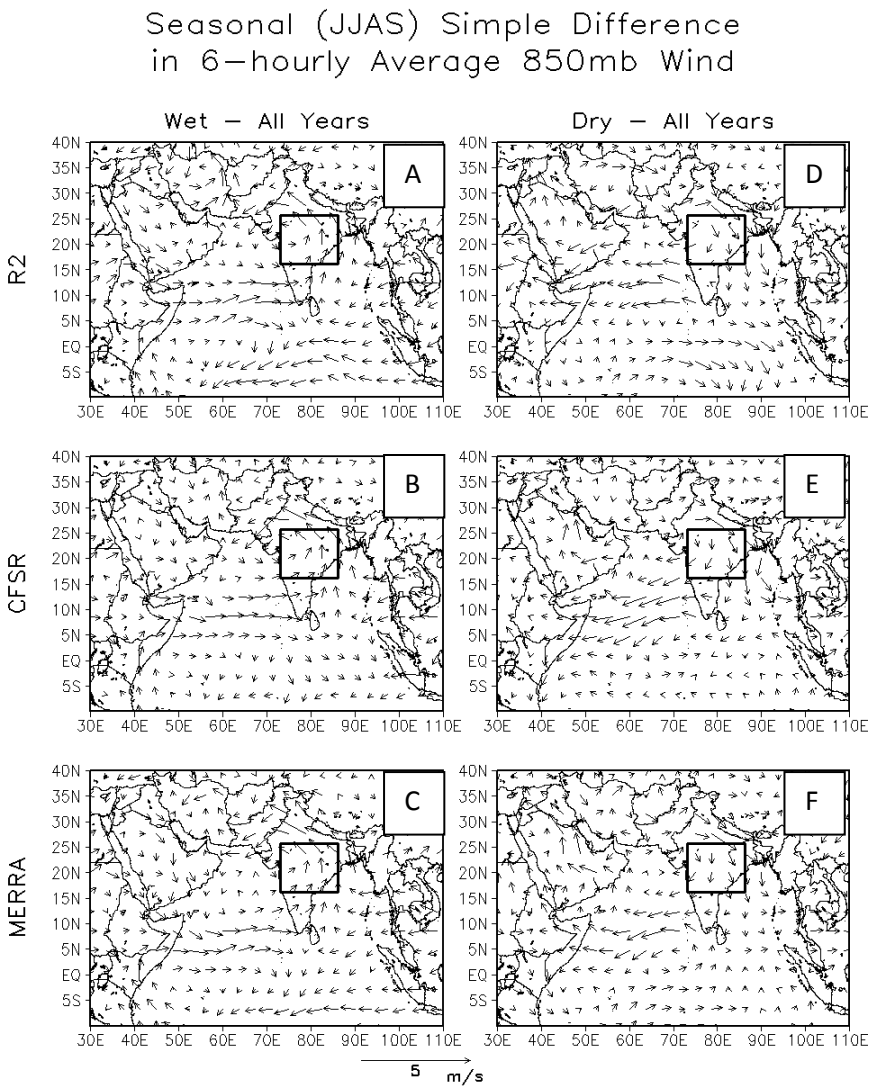

Figure 4-6. Simple difference in the six-hourly average 850 mb wind fields between wet years and all years for R2 (a), CFSR (b), and MERRA (c) and then for dry years and all years for R2 (d), CFSR (e), and MERRA (f). Scale is shown at the bottom of the figure.

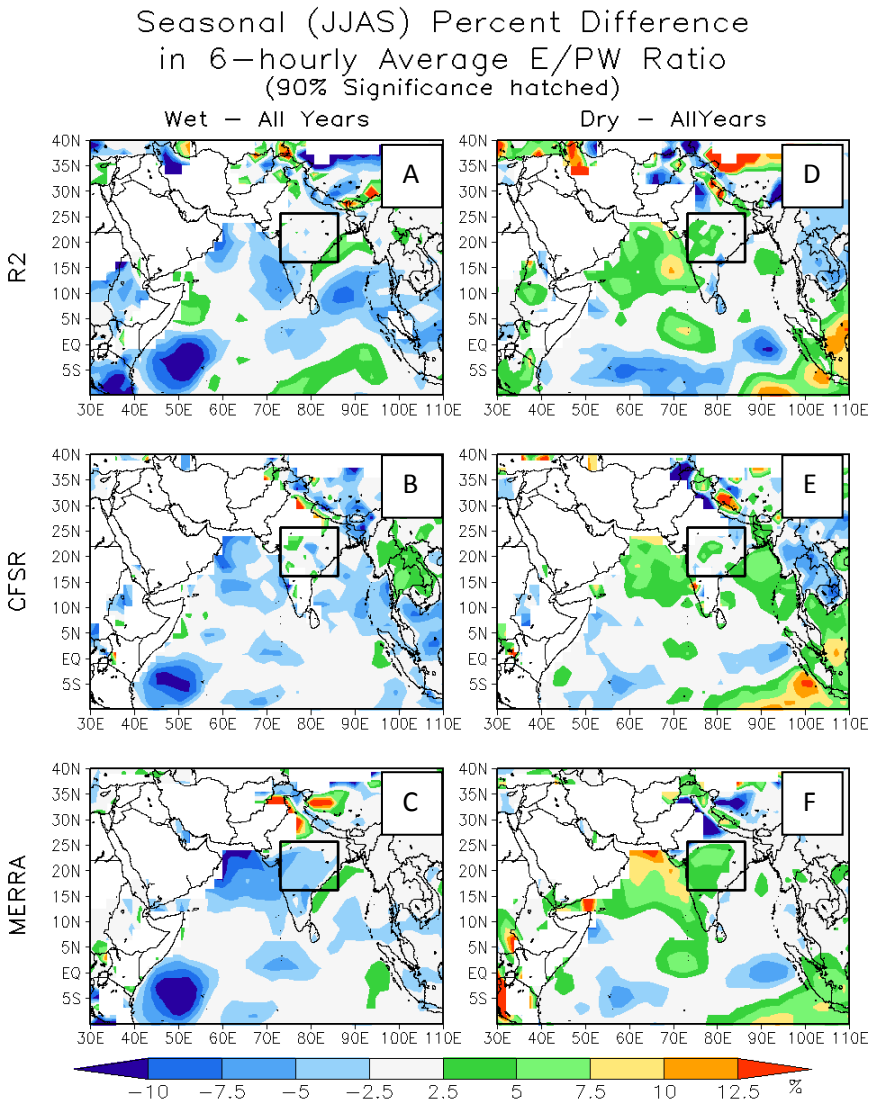

Figure 4-7. Same as Figure 4-6, but showing the percentage difference in six-hourly average $\frac{E}{PW}$ ratio. Here, areas of 90% significance are hatched. Areas of low ratio (< 5%) are masked out.

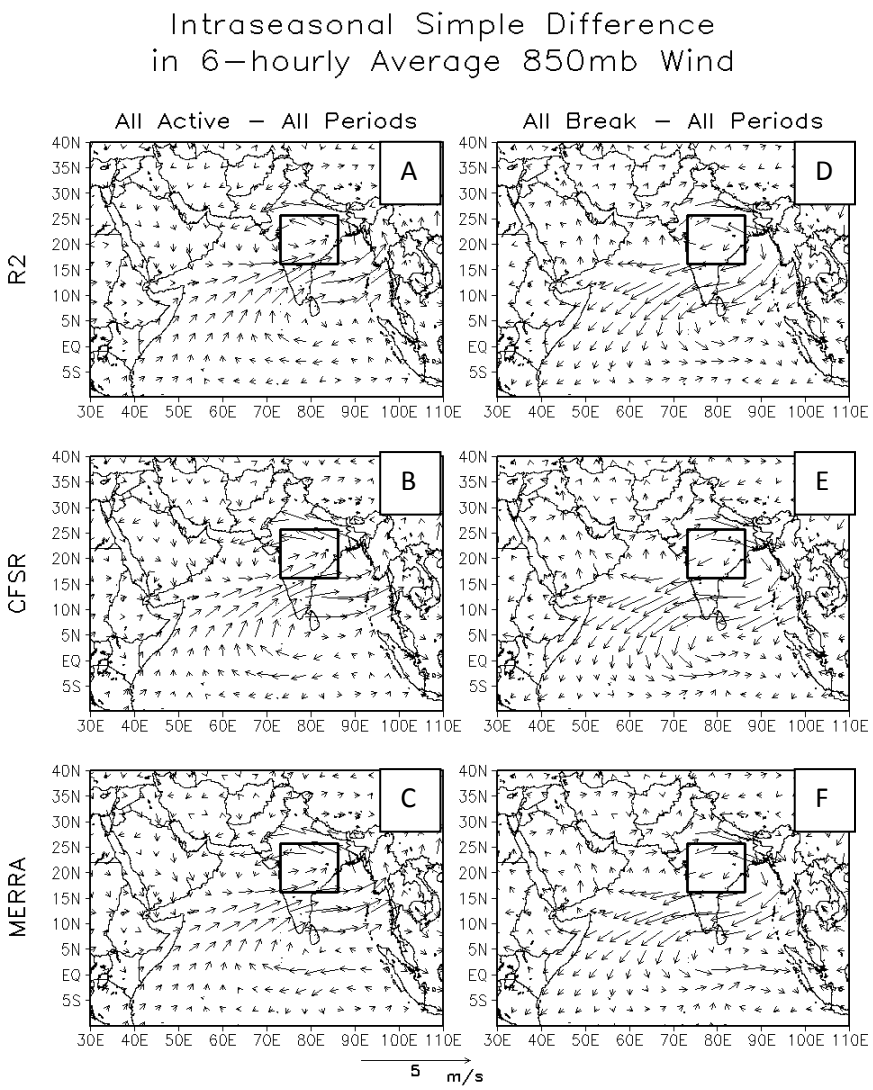

Figure 4-8. Same as Figure 4-6, but between active periods and all periods (a–c) and break periods and all periods (d–f).

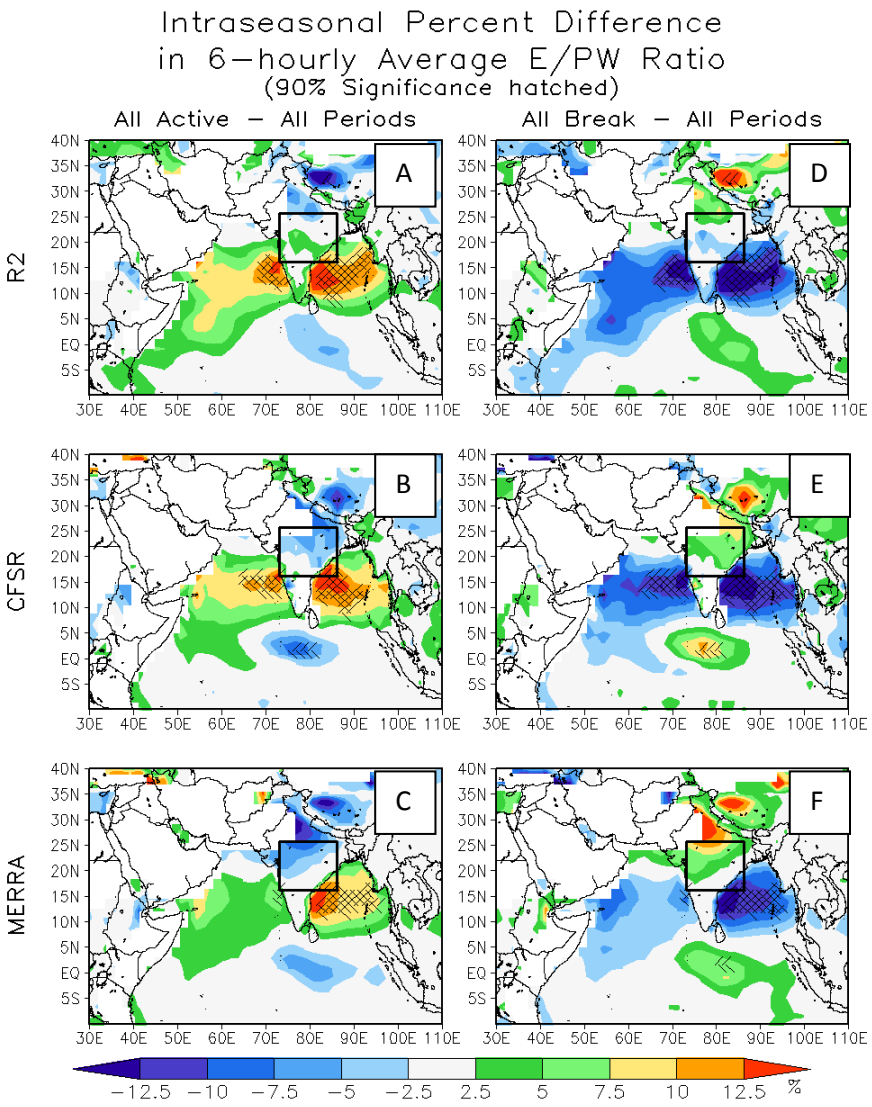

Figure 4-9. Same as Figure 4-7, but between active periods and all periods (a–c) and break periods and all periods (d–f).

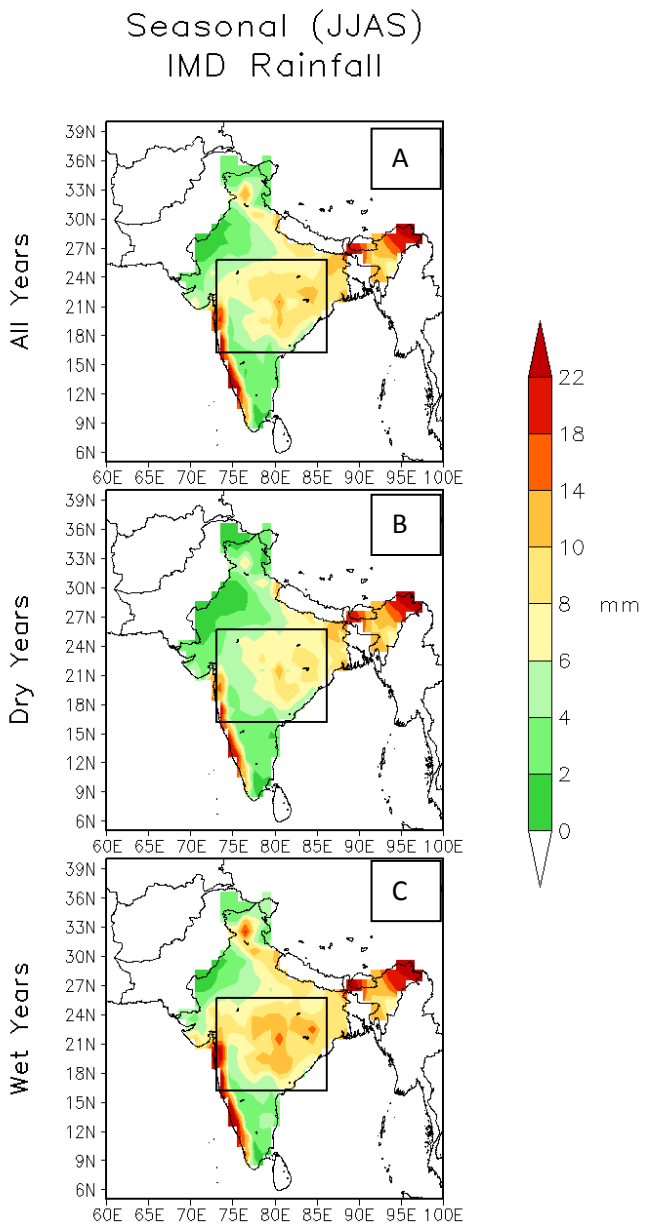

Figure 4-10. Daily-average seasonal IMD gridded rainfall over India for all 15 years (a), all dry years (b), and all wet years (c).

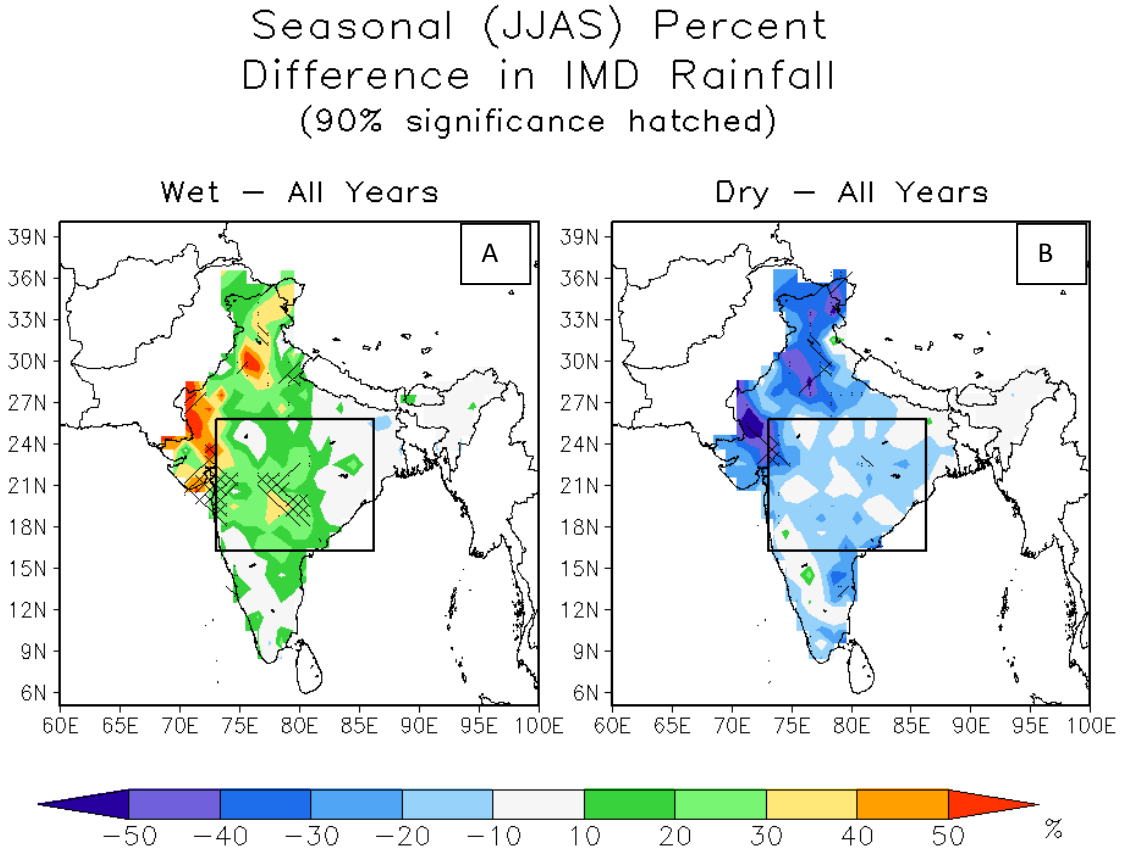

Figure 4-11. Daily-average seasonal IMD gridded rainfall percentage differences between wet years and all years (a), and dry years and all years (b). Areas of 90% significance are hatched.

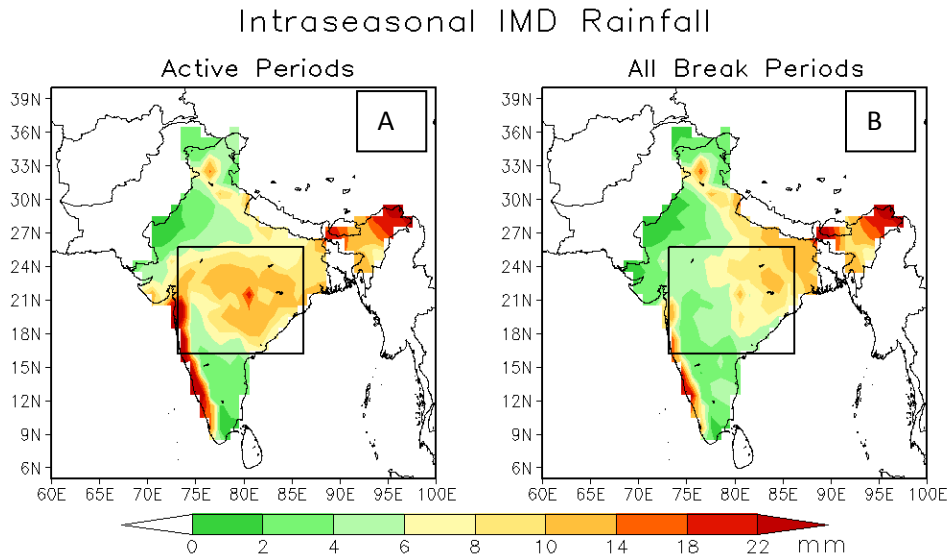

Figure 4-12. Daily-average IMD gridded rainfall for active periods from all years (a) and break periods from all years (b). These represent a composite of all specified periods, which may range in length from 10 to 30 days.

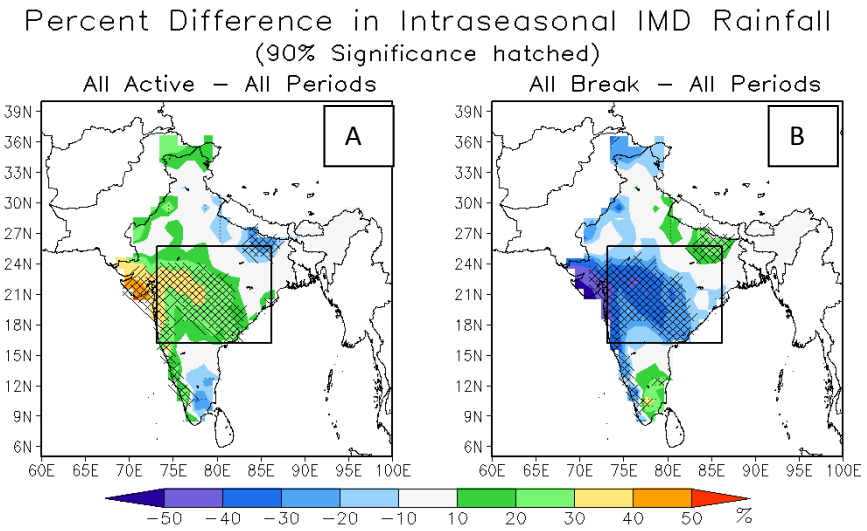

Figure 4-13. Percentage difference in daily-average IMD gridded rainfall between active periods from all years and all periods (a) and break periods from all years and all periods (b). Areas of 90% significance are hatched.

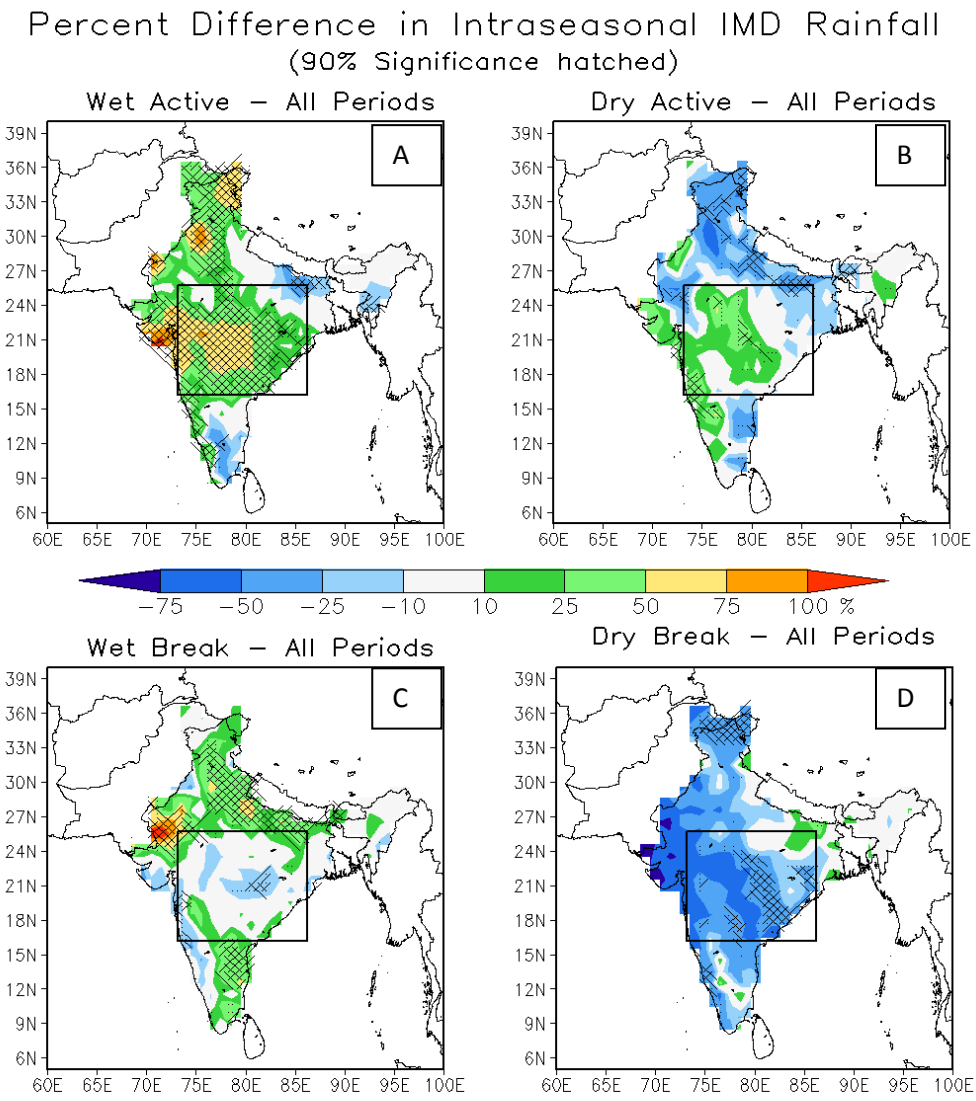

Figure 4-14. Percentage difference in daily-average IMD gridded rainfall between active periods from wet years and all periods (a), break periods from wet years (b), active periods from dry years (c), and break periods from dry years (d). Areas of 90% significance are hatched.

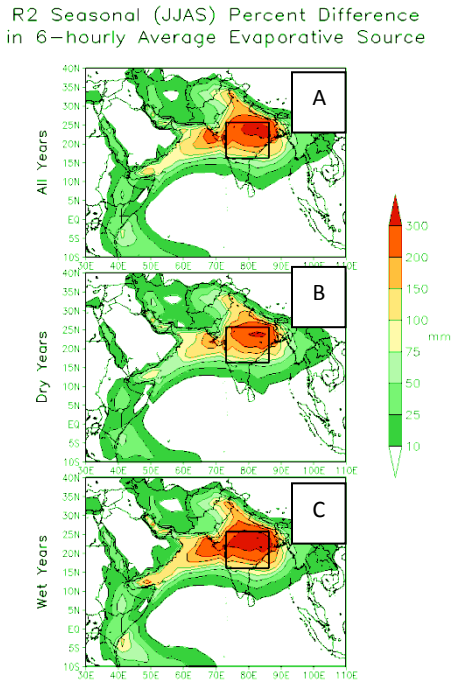

Figure 4-15. Seasonal (JJAS) six-hourly average total evaporative source as estimated by R2 in all years (17a), dry years (17b), and wet years (17c)

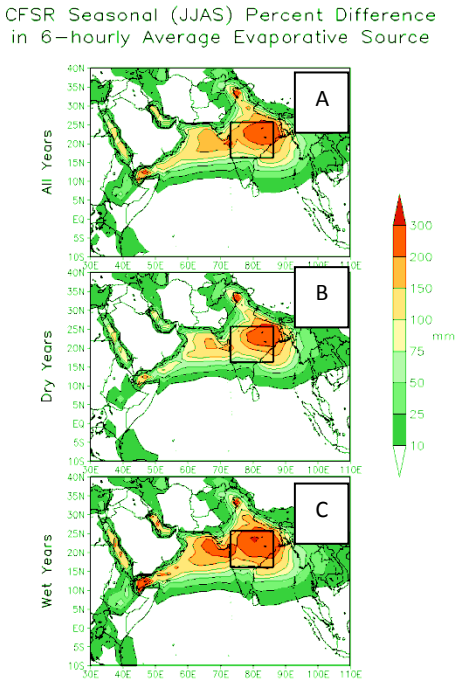

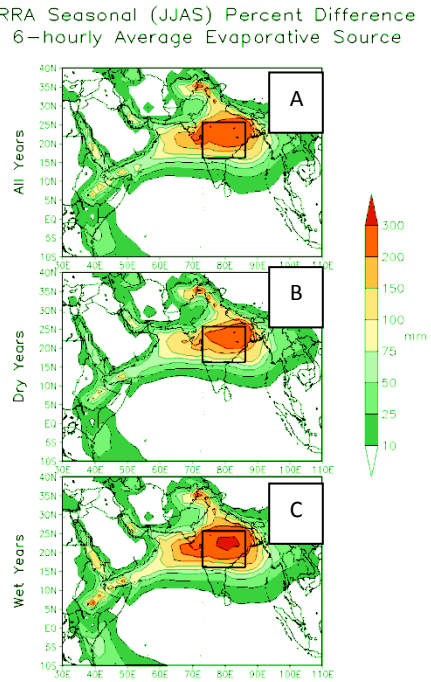

Figure 4-16. (left) Same as Figure 4-15 but for CFSR.
Figure 4-17. (right) Same as Figure 4-15 but for MERRA.

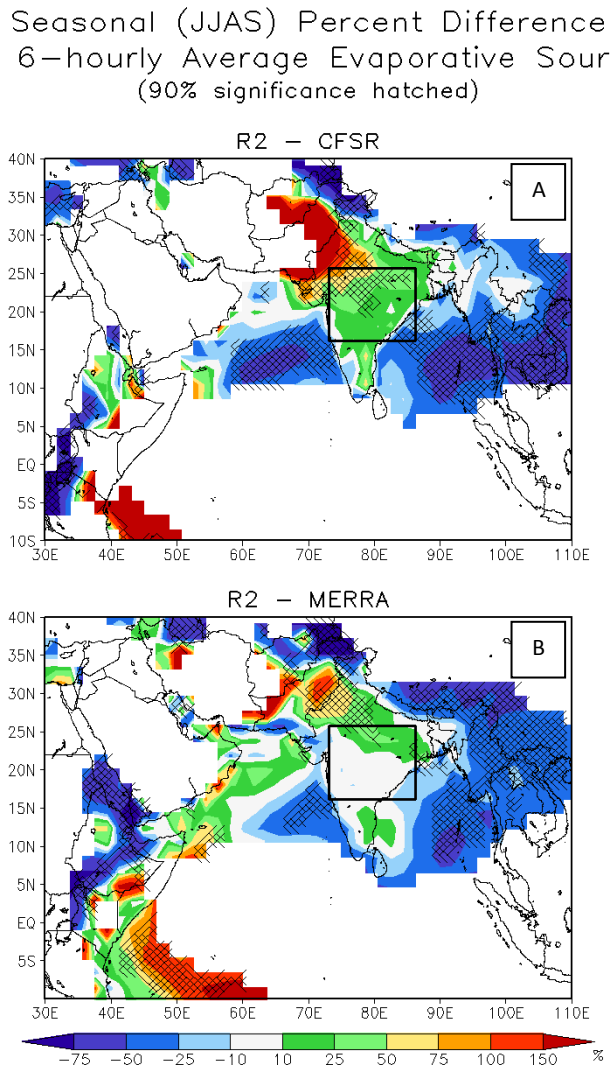

Figure 4-18. Percentage difference in seasonal six-hourly average evaporative source between R2 and CFSR in all years (a) and between R2 and MERRA in all years (b). Areas of 90% significance are hatched. Areas of low (< 5 mm) evaporative source are masked out.

Table 4-1. This table shows the recycling ratio of evaporative source for all years, wet years, and dry years. The recycling ratio is given by the fraction of evaporative source that exists over the central India region over the evaporative source that exists over the entire domain (30°E – 110 °E and -10 °S – 40 °N).

Local-to-remote Moisture Ratio			
	R2	**CFSR**	**MERRA**
All Years	31.5	28.2	29.4
Wet Years	37.0	33.1	33.9
Dry Years	26.7	24.8	25.4

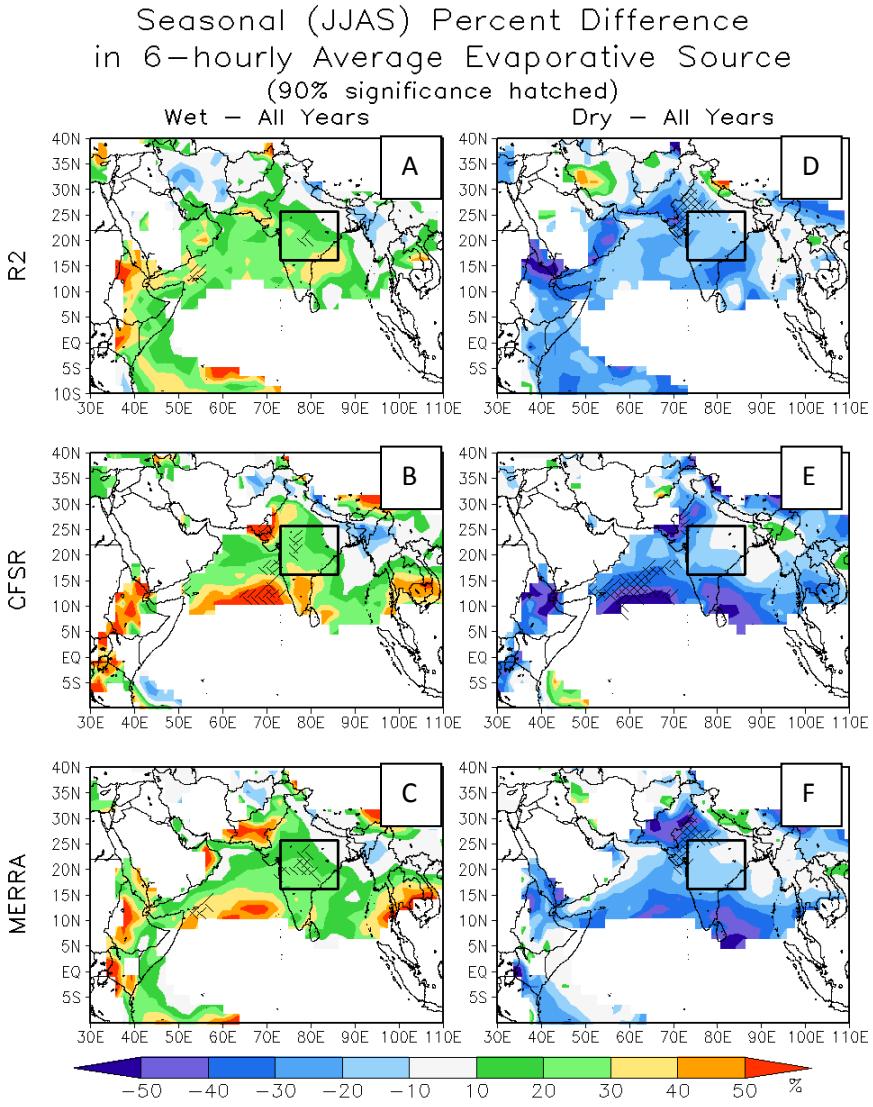

Figure 4-19. Percentage difference in six-hourly average evaporative source between wet years and all years for R2 (a), CFSR (b), and MERRA (c), and between dry years and all years for R2 (d), CFSR (e), and MERRA (f). Areas of 90% significance are hatched. Areas of low (< 5 mm) evaporative source are masked out.

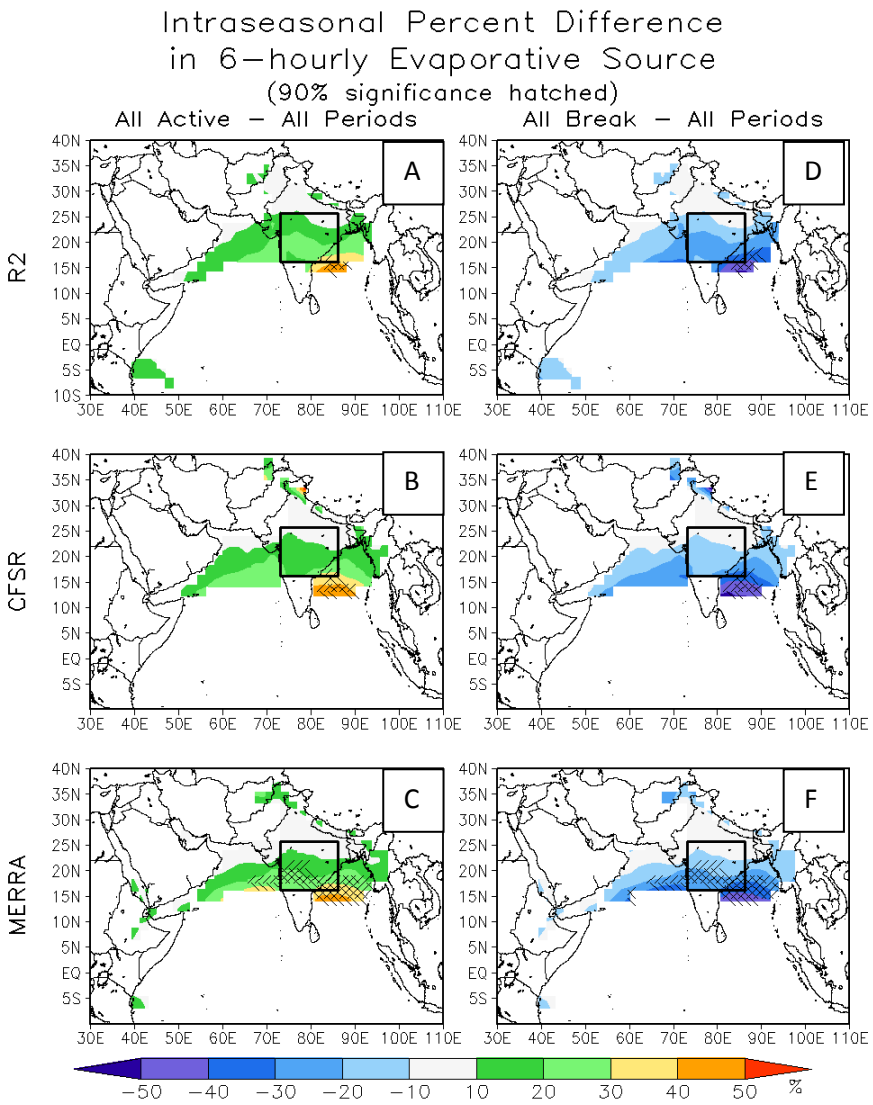

Figure 4-20. Same as Figure 4-19, but for all active periods from all years (a–c) and all break periods from all years (d–f).

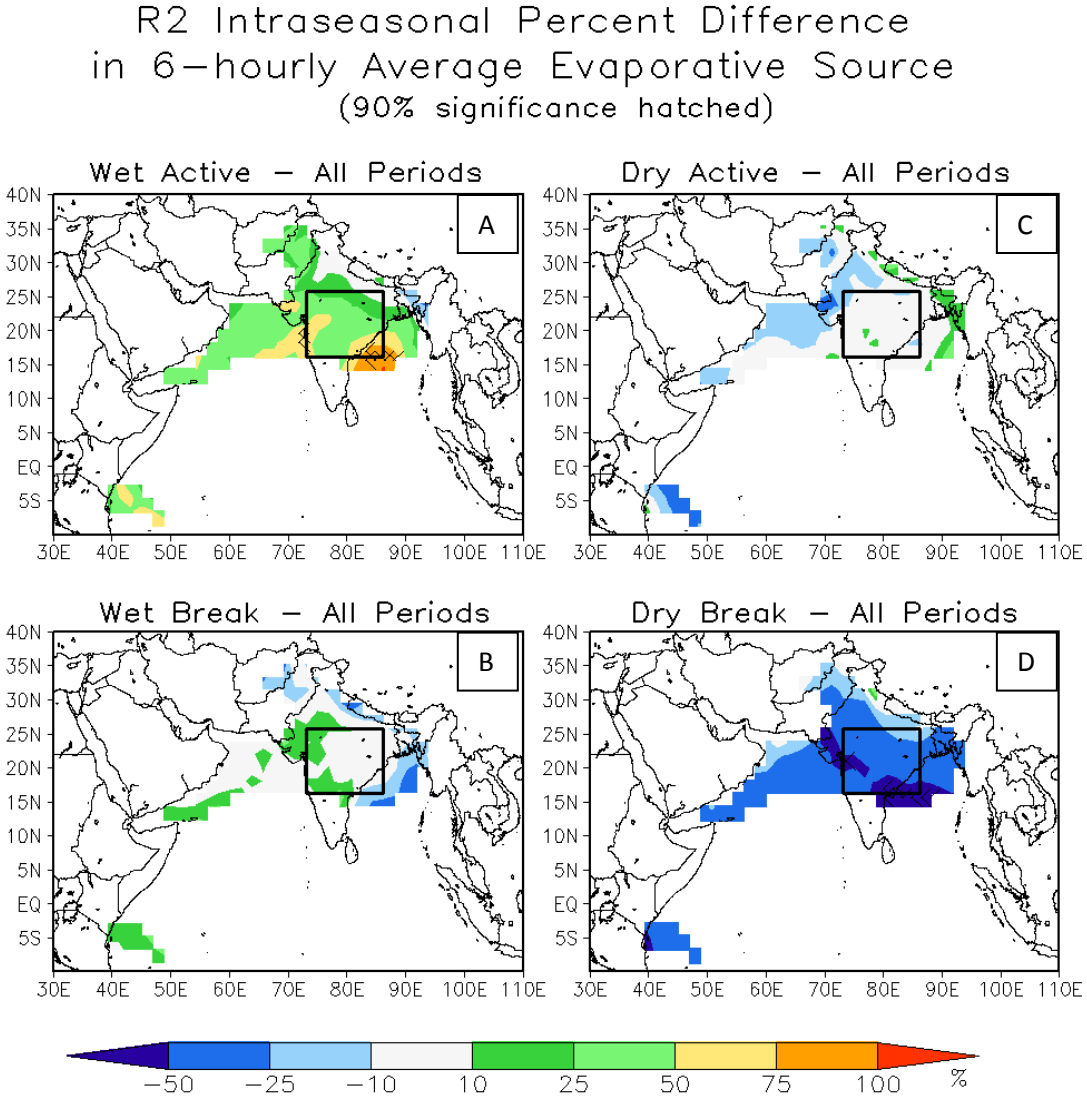

Figure 4-21. Percentage difference in six-hourly average evaporative source between active periods from wet years and all periods (a), break periods from wet years and all periods (b), active periods from dry years and all periods (c), and break periods from dry years (d) for R2. Areas of 90% significance are hatched. Areas of low (< 5 mm) evaporative source are masked out.

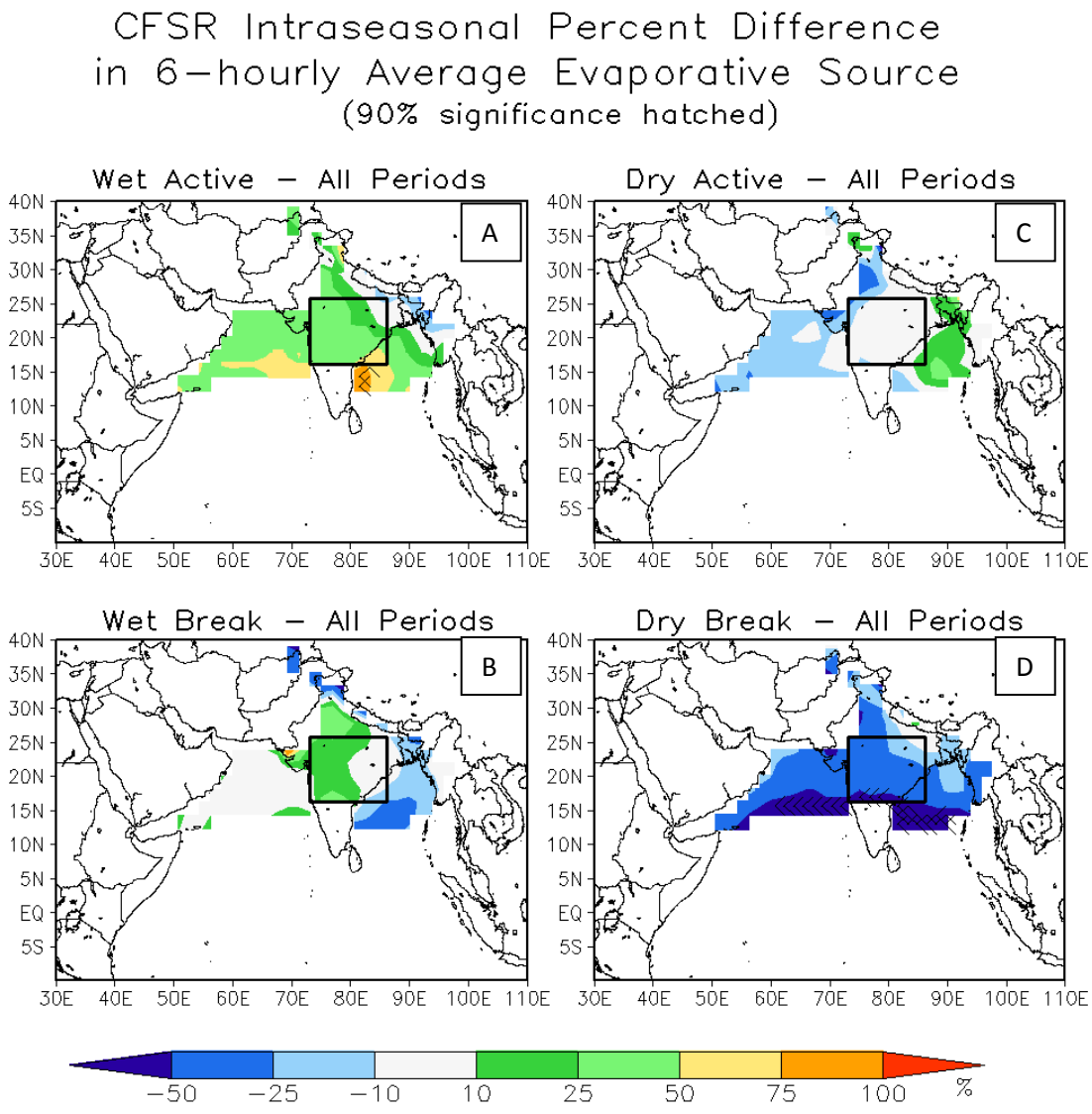

Figure 4-22. Same as Figure 4-21 but for CFSR.

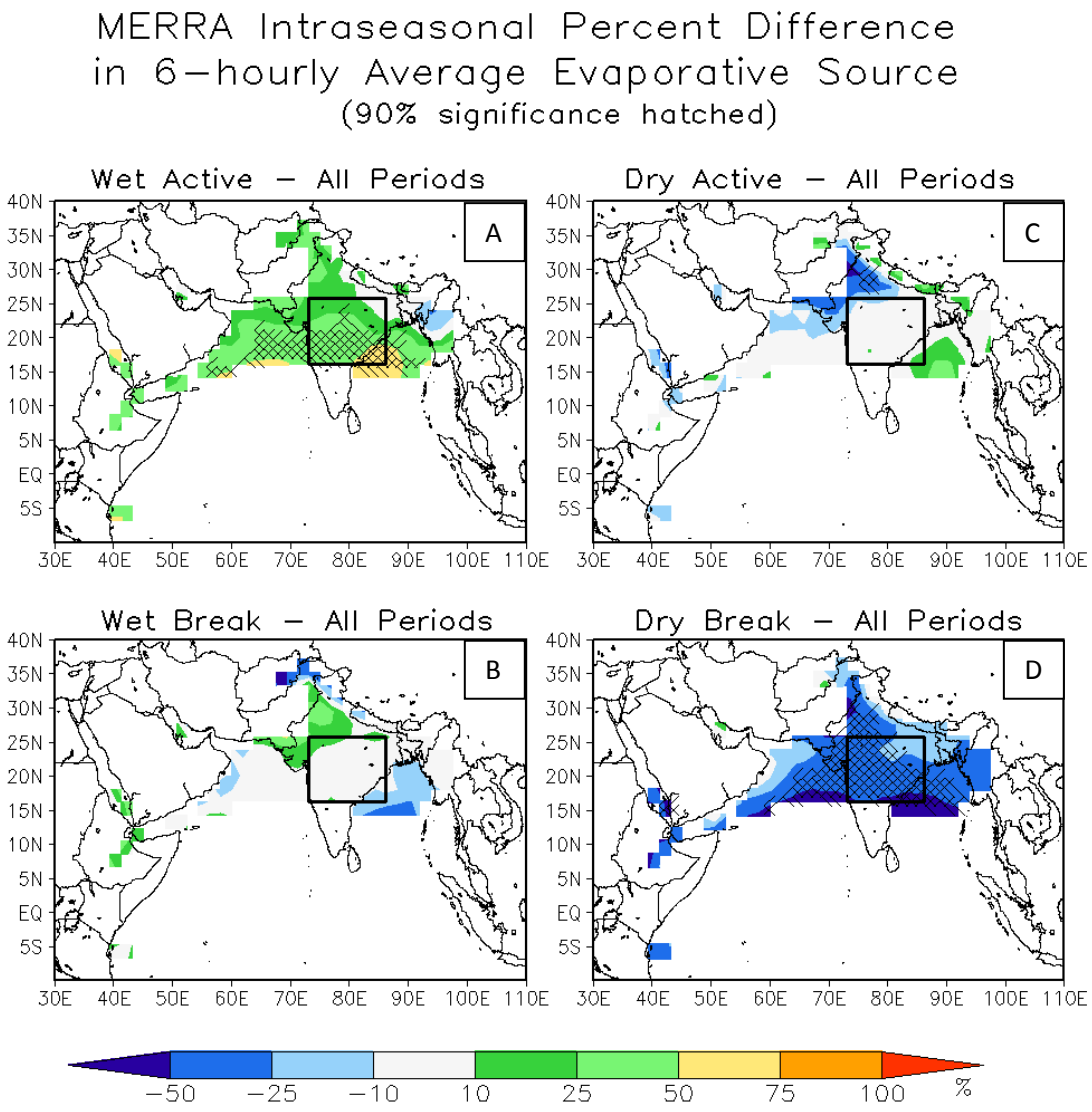

Figure 4-23. Same as Figure 4-21 but for MERRA.

CHAPTER FIVE
CONCLUSIONS

In this study, we isolated interannual and intraseasonal changes in the location and magnitude of evaporative sources for rainfall events during the summertime Indian monsoon, and we intended to improve our understanding of the variability of the monsoon. Overall, we accomplished several of the goals laid out in the initial part of this study.

We found that there are significant differences in the evaporation, wind, and PW fields from R2, CFSR, and MERRA. R2 features higher evaporation rates over land compared to CFSR or MERRA. The 850 mb winds tend to be stronger in R2 than in CFSR. The cross-equatorial flow region is enhanced (reduced) during wet (dry) years as well as active (break) periods compared to average. The PW values tend to be lower (higher) in R2 than in either CFSR or MERRA over eastern India and the Bay of Bengal (eastern Africa). The $\frac{E}{PW}$ ratio reflects changes in both of the fields and varies on interannual and intraseasonal time scales.

We also confirmed that our methods used to isolate interannual and intraseasonal variability in the rainfall were sufficient. Our defined wet years/active periods are significantly wetter than average. Our differences on the intraseasonal time scale are more robust due to a larger sample size.

Finally, we traced the evaporative sources interannually and intraseasonally. We found that *all datasets produce similar plots for seasonal evaporative source* and generally concentrated it locally over central India. R2 generally produces more local evaporative source over land compared to CFSR and MERRA, which feature larger remote influences of the water and its associated moisture.

The *location and strength of the evaporative source for interannual rainfall events changes most significantly over the central India and parts of the Arabian Sea in all three datasets*, which suggests changes in the character of the overall monsoon circulation and the cross-equatorial flow. We saw an enhancement in evaporative source for wet years and a reduction in evaporative source in dry years. *The location and strength of the evaporative source*

for intraseasonal rainfall events changes most significantly over the northeastern Bay of Bengal in all three datasets, which suggests the influence of landfalling TCs and low pressure systems in supplying moisture to the region in active periods. We saw an enhancement of the evaporative source for all active periods and a reduction in evaporative source for all dry periods. The location and strength of the evaporative sources for intraseasonal events are also influenced on an interannual timescale. We found a large *enhancement in evaporative source over the Bay of Bengal, the Arabian Sea, and most of India during active periods from wet years and a reduction in evaporative source over those same regions in break periods from dry years*. However, active periods from dry years and break periods from wet years draw their moisture from sources that are different that in active periods from wet years and break periods from dry years, respectively.

We concluded that a combination of precipitation rates, moisture availability, and winds plays the largest role in dictating the characteristics of the evaporative source for the monsoon rainfall. In cases for which we did not vary the input rainfall dataset, $\frac{E}{PW}$ ratio and winds had the largest influence on the local and remote nature of evaporative source.

We observed that the dominant changes in the location of the evaporative sources on interannual and intraseasonal time scales are not collocated. This result has implications for climate predictability over the Indian monsoon region. Although there is current interest in improving the interannual predictability of the monsoon, we require an improvement in the intraseasonal to improve overall predictability. We suggest in this study that models need improved estimates of the moisture fields and atmospheric water content, both over the Bay of Bengal and the Arabian Sea, to accomplish reliable predictability.

Several limitations exist within this study. Our analysis relies on just fifteen years of data and five years each for the wet and dry cases. This is a necessary consequence of our dataset being limited to the period between 1979 and 2003, but the fact remains that larger sample sizes would provide greater significance and more validity to our results. We also have clearly identified any physical mechanisms to explain the interannual or intraseasonal variability of evaporative source other than the differences in the evaporation, PW, and wind parameters outlined above. Differences in the fields of vorticity, outgoing long-wave radiation (OLR), or upper level winds have been documented in monsoon literature and could also be compared among our datasets to help isolate changes in the evaporative source on these time scales. Also, circulation changes such as those described for ENSO, the TBO, or TC presence could be

specifically studied to see if they are the main causes of the changes in flow that we observe at different time scales. We could attempt to isolate the changes in each of the parameters during the interannual changes of the ISOs; these were omitted for this study in the interest of conciseness.

On scales beyond the purview of this study, more research is necessary to accurately depict the variation of the monsoon. Although several mechanisms were outlined in Chapter 1 to explain interannual and intraseasonal variability, much debate remains regarding the overall contribution of each mechanism to total variability of the monsoon. Furthermore, the QIBT used in this study has obvious limitations (Chapter 2), and the program's code itself can be modified to introduce sources and sinks of moisture other than the ones previously described. This would provide a more accurate representation of the evaporation sources we wish to trace.

Opportunities for future research also exist within this study. It would be helpful to use EOF analysis as cited in the literature to identify the main modes of variability in the interannual and intraseasonal evaporative sources. This would allow us to document the dominant features of the variance in this parameter and would help us to compare and contrast it to the modes of variability of Indian rainfall that are well documented in the literature. However, a larger sample size is required before we complete this task with confidence. This study could be altered to compare seasonal variability of the monsoon on other time scales, such as that of ENSO. It is clear that ENSO and the monsoon are strongly influenced by one another, so it would be interesting to note changes in the evaporative source character due to these interactions. Finally, our QIBT could be used to trace the evaporative source for monsoon systems across the globe and could serve as a proxy method to study transport of dust, pollutants, pathogens, or aerosols from one location to another. One such study will attempt to monitor the source regions for dust particles moving over the southeastern U.S. from the coast of Africa. Pathogens are known to attach to these particles and become introduced to remote regions via this mode of transport. It would be interesting to note changes in dust source regions to improve studies of climatology and associated epidemiology over western Africa and to expand this line of research far beyond its initial intentions.

APPENDIX A

DATE TABLES

Table A-1. List of the starting and ending dates for each of the active periods we isolated from all years (56 total). These were converted to pentad dates for the purposes of this study. An active period is defined as 10–30 days of above average (filtered) rainfall

Active Periods			
Start Date	**End Date**	**Start Date**	**End Date**
15jun1979	29jun1979	14jul1988	07aug1988
30jul1979	13aug1979	18aug1988	01sep1988
29aug1979	12sep1979	17sep1988	26sep1988
13sep1979	27sep1979	05jun1989	04jul1989
05jun1982	24jun1982	15jul1989	29jul1989
15jul1982	29jul1982	14aug1989	28aug1989
09aug1982	23aug1982	18sep1989	02oct1989
08sep1982	27sep1982	10jun1990	04jul1990
20jun1983	04jul1983	15jul1990	24jul1990
04aug1983	18aug1983	09aug1990	23aug1990
03sep1983	17sep1983	18sep1990	02oct1990
04jun1984	18jun1984	10jun1994	24jun1994
29jun1984	13jul1984	05jul1994	19jul1994
03aug1984	17aug1984	24aug1994	07sep1994
07sep1984	16sep1984	09jun1996	23jun1996
31may1985	14jun1985	19jul1996	07aug1996
15jun1985	29jun1985	18aug1996	16sep1996
25jul1985	13aug1985	15jun1997	04jul1997
03sep1985	17sep1985	25jul1997	03aug1997
15jun1986	29jun1986	19aug1997	02sep1997
15jul1986	24jul1986	13sep1997	27sep1997
04aug1986	18aug1986	10jun1998	19jun1998
08sep1986	22sep1986	30jun1998	14jul1998
05jun1987	14jun1987	30jul1998	18aug1998
30jun1987	14jul1987	08sep1998	17sep1998
19aug1987	02sep1987	15jun2002	29jun2002
13sep1987	22sep1987	04aug2002	18aug2002
04jun1988	28jun1988	18sep2002	02oct2002

Table A-2. Same as Table A-1 but for all break periods (49 total).

Break Periods			
Start Date	**End Date**	**Start Date**	**End Date**
30jun1979	29jul1979	02sep1988	16sep1988
14aug1979	28aug1979	05jul1989	14jul1989
25jun1982	14jul1982	30jul1989	13aug1989
30jul1982	08aug1982	29aug1989	17sep1989
24aug1982	07sep1982	05jul1990	14jul1990
05jul1983	19jul1983	25jul1990	08aug1990
19aug1983	02sep1983	24aug1990	17sep1990
18sep1983	02oct1983	25jun1994	04jul1994
18jun1984	28jun1984	20jul1994	03aug1994
14jul1984	02aug1984	04aug1994	23aug1994
18aug1984	06sep1984	08sep1994	27sep1994
17sep1984	01oct1984	24jun1996	18jul1996
30jun1985	24jul1985	03aug1996	17aug1996
14aug1985	02sep1985	17sep1996	01oct1996
18sep1985	02oct1985	05jul1997	24jul1997
30jun1986	14jul1986	04aug1997	18aug1997
25jul1986	03aug1986	03sep1997	12sep1997
19aug1986	07sep1986	15jul1998	29jul1998
23sep1986	02oct1986	19aug1998	07sep1998
15jun1987	29jun1987	18sep1998	02oct1998
15jul1987	13aug1987	30jun2002	14jul2002
03sep1987	12sep1987	20jul2002	03aug2002
23sep1987	02oct1987	19aug2002	28aug2002
29jun1988	13jul1988	08sep2002	17sep2002
08aug1988	17aug1988		

Table A-3. List of all dates within the timeframe of the study along with their associated pentad-day. Note how the occurrence of a leap year results in the addition of one Julian day to the calendar and also shifts the dates of interest compared to those of a non-leap year.

Pentad Number for Summertime Dates												
Pentad	No Leap Year						Leap Year					
	Julian Day	Dates					Julian Day	Dates				
30	146	5/26	5/25	5/26	5/27	5/28	147	5/25	5/26	5/27	5/28	5/29
31	151	5/31	5/30	5/31	6/1	6/2	152	5/30	5/31	6/1	6/2	6/3
32	156	6/5	6/4	6/5	6/6	6/7	157	6/4	6/5	6/6	6/7	6/8
33	161	6/10	6/9	6/10	6/11	6/12	162	6/9	6/10	6/11	6/12	6/13
34	166	6/15	6/14	6/15	6/16	6/17	167	6/14	6/15	6/16	6/17	6/18
35	171	6/20	6/19	6/20	6/21	6/22	172	6/19	6/20	6/21	6/22	6/23
36	176	6/25	6/24	6/25	6/26	6/27	177	6/24	6/25	6/26	6/27	6/28
37	181	6/30	6/29	6/30	7/1	7/2	182	6/29	6/30	7/1	7/2	7/3
38	186	7/5	7/4	7/5	7/6	7/7	187	7/4	7/5	7/6	7/7	7/8
39	191	7/10	7/9	7/10	7/11	7/12	192	7/9	7/10	7/11	7/12	7/13
40	196	7/15	7/14	7/15	7/16	7/17	197	7/14	7/15	7/16	7/17	7/18
41	201	7/20	7/19	7/20	7/21	7/22	202	7/19	7/20	7/21	7/22	7/23
42	206	7/25	7/24	7/25	7/26	7/27	207	7/24	7/25	7/26	7/27	7/28
43	211	7/30	7/29	7/30	7/31	8/1	212	7/29	7/30	7/31	8/1	8/2
44	216	8/4	8/3	8/4	8/5	8/6	217	8/3	8/4	8/5	8/6	8/7
45	221	8/9	8/8	8/9	8/10	8/11	222	8/8	8/9	8/10	8/11	8/12
46	226	8/14	8/13	8/14	8/15	8/16	227	8/13	8/14	8/15	8/16	8/17
47	231	8/19	8/18	8/19	8/20	8/21	232	8/18	8/19	8/20	8/21	8/22
48	236	8/24	8/23	8/24	8/25	8/26	237	8/23	8/24	8/25	8/26	8/27
49	241	8/29	8/28	8/29	8/30	8/31	242	8/28	8/29	8/30	8/31	9/1
50	246	9/3	9/2	9/3	9/4	9/5	247	9/2	9/3	9/4	9/5	9/6
51	251	9/8	9/7	9/8	9/9	9/10	252	9/7	9/8	9/9	9/10	9/11
52	256	9/13	9/12	9/13	9/14	9/15	257	9/12	9/13	9/14	9/15	9/16
53	261	9/18	9/17	9/18	9/19	9/20	262	9/17	9/18	9/19	9/20	9/21
54	266	9/23	9/22	9/23	9/24	9/25	267	9/22	9/23	9/24	9/25	9/26
55	271	9/28	9/27	9/28	9/29	9/30	272	9/27	9/28	9/29	9/30	10/1
56	276	10/3	10/2	10/3	10/4	10/5	277	10/2	10/3	10/4	10/5	10/6

REFERENCES

Arpe, K., et al., 1998. Variability of the Indian monsoon in the ECHAM3 model: Sensitivity to sea surface temperature, soil moisture, and the stratospheric quasi-biennial oscillation. *J. Climate*, **11**, 1837–1858.

Bamzai, A.S., and J. Shukla, 1999. Relation between Eurasian Snow Cover, Snow Depth, and the Indian Summer Monsoon: An Observational Study. *J. Climate*, **12**, 3117-3132.

Beck, C. et al., 2005. A new monthly precipitation climatology for the global land area for the period 1951 to 2000. *Climate Status Report 2004*, 181 – 190.

Beljaars, A. C., et al., 1996. The anomalous rainfall over the United States during July 1993: Sensitivity to land surface parameterization and soil moisture anomalies. *Mon. Wea. Rev.*, **124**, 362-383.

Benton, G. S., et al., 1950. The role of the atmosphere in the hydroplogic cycle. *Trans. Am. Geophsyc. Union*, **31**, 61–73.

Bosilovich, M. G., et al., 2008: Evaluation of precipitation in reanalyses. *J. Appl. Meteorol. and Climatol*., **47**, 2279–2299.

Budyko, M. I., 1974. Climate and Life. *Academic Press*, 508pp.

Brubaker, K. L., et al., 1993. Estimation of continental precipitation recycling. *J. Climate*, **6**, 1077–1089.

Cadet, D., and G. Reverdin, 1981. Water vapour transport over the Indian Ocean during summer 1975. *Tellus*, **33**, 476–487.

Chan, S. C., and V. Misra, 2009. A diagnosis of the 1979-2005 extreme rainfall events in the Southeast US with isentropic moisture tracing. *Mon. Wea. Rev.*¸ **138**, 1172-1185.

Chen, J. and M. G. Bosilovich, 2008. A preliminary study of global water and energy cycles in a NASA reanalysis system. *20th Conference on Climate Variability and Change*.

Dirmeyer, P.A., 2000. Using a global soil wetness dataset to improve seasonal climate simulation. *J. Climate*, **13**, 2900-2922.

_____, P. A. and K. L. Brubaker, 1999. Contrasting evaporative moisture sources during the drought of 1988 and the flood of 1993. *J. of Geophysical Res.*, **104,** 19383-19397.

_____, and _____, 2007. Characterization of the global hydrologic cycle from a back-trajectory analysis of atmospheric water vapor. *J. Hydrometeor*, **8**, 20–37.

Fasullo, J., 2004: Biennial characteristics of Indian monsoon rainfall. *J. Climate*, **17**, 2972–2982.

Gadgil, S., 2003. The Indian monsoon and its variability. *Annu. Rev. Earth Planet. Sci.*, **31**, 429-467.

Goswami, B. N., and R. S. Ajaya Mohan, 2001. Intraseasonal oscillations and interannual variability of the Indian monsoon. *J. Climate*, **14**, 1180-1198.

_____, et al., 2003. Clustering of synoptic activity by Indian summer monsoon intraseasonal oscillations. *Geophysical Research Letters*, **30**, 14-1 – 14-4.

_____, et al., 2008. Intraseasonal variability and forecasting: A review of recent research. *Forth Annual Workshop on Monsoons.*

Herndon, H. H., et al.,1999. Interannual variation of the Madden-Julian oscillation during austral summer. *J. Climate,* **12**, 2538–2550..

Higgins, R. W., et al., 2010. Intercomparison of daily precipitation statistics over the United States in observations and in NCEP reanalysis products. *J. Climate*, **23**, 4637-4650.

Jones, C., et al., 2004. Climatology of tropical intraseasonal convection anomalies: 1979-2002. *J. Climate*, **17**, 523-539.

Joyce, R. J., et al., 2004: CMORPH: A method that produces global precipitation estimates from passive microwave and infrared data at high spatial and temporal resolution. *J. Hydrometeor*, **5**, 487–503.

Kalnay, E., et al., 1996. The NCEP/NCAR 40-year reanalysis project. *Bull. Amer. Meteor. Soc.*, **77,** 437-471.

Kanamitsu, M., et al., 2002. NCEP-DOE AMIP-II Reanalysis (R-2). *Bull. Amer. Meteor. Soc.*, **83**, 1631-1643.

Kerr, J. M., 1996. Sustainable development of rainfed agriculture in India. *EPTD Discussion Paper No. 20*.

Kirtman and Shukla, 2000. Influence of the Indian summer monsoon on ENSO. *Q. J. R. Meteorl. Soc.*, **126**, 213–239.

Koster, R. D., et al., 2004. Regions of strong coupling between soil moisture and precipitation. *Science*, **305**, 1138–1140.

Krishna Kumar, K., et al., 1999. On the weakening relationship between the Indian monsoon and ENSO. *Science*, **284**, 2156–2159.

Krishnamurthy V., and J. Shukla, 2000. Intraseasonal and interannual variability of rainfall over India. *J. Climate*, **13**, 4366-4377.

_____, and ____, 2006. Intraseasonal and seasonally persisting patterns of Indian monsoon rainfall. *J. Climate*, **20**, 3-20.

_____, and J. L. Kinter, 2003. The Indian monsoon and its relation to global climate variability. *Global Climate.*

Krishnamurti, T. N., et al, 1995. Predictions of Dry and Wet spell of the Australian Monsoon. *International Journal of climatology*, **15**, 753-771.

Kumar, S. V., et al., 2008. A land surface data assimilation framework using the land information system: Description and application. *Advances in Water Resources*, **31**, 1419–1432.

Lau, K-M., et al., 2000: Dynamical and boundary forcing characteristics of regional components of the Asian summer monsoon. *J. Climate*, **13**, 2461–2482.

Lawrence, D. M. and P. J. Webster, 2001. Interannual variations of the intraseasonal oscillation in the South Asian summer monsoon region. *J. Climate*, **14**, 2910-2922.

Lim, Y. K., et al., 2002. Temporal and spatial evolution of the Asian summer monsoon in the seasonal cycle of synoptic fields. *J. Climate*, **15**, 3630–3644.

Maurer, E. P., et al., 2000. Evaluation of the land surface water budget in NCEP/NCAR and NCEP/DOE AMIP-II reanalyses using an off-line hydrologic model. *J. Geophys. Res.*, **106** (D16), 17841-17862.

Meehl 1994: Coupled land–ocean–atmosphere processes and south Asian monsoon variability. *Science*, **266**, 263–267.

_____, Gerald A., 1997: The South Asian Monsoon and the Tropospheric Biennial Oscillation. *J. Climate*, **10**, 1921–1943.

Mooley, D. A., and B. Parthasarathy, 1984. Fluctuations in All-India summer monsoon rainfall during 1871-1978. *Climate Change*, **6**, 287-301.

Nigam, S., and A. Ruiz-Barradas, 2006. Seasonal hydroclimate variability over North America in global and regional reanalyses and AMIP simulations: Varied representation. *J. Climate*, **15**, 815-837.

Paegle, J. et al., 1996. Dependence of simulated precipitation on surface evaporation during the 1993 United States summer floods. *Mon. Wea. Rev*., **124**, 345–361.

Rajeevan, M., et al., 2006. High resolution daily gridded rainfall data for the Indian region: Analysis of break and active monsoon spells. *Curr. Sci.*, **91**, 296-306.

Ruiz-Barradas, A., and S. Nigam, 2004. Warm season rainfall variability over the US Great Plains in observations, NCEP and ERA-40 reanalyses, and NCAR and NASA atmospheric model simulations. *J. Climate*, **18**, 1808-1830.

Saha, S., et al., 2010. The NCEP Climate Forecast Reanalysis. *Bull. Amer. Meteor. Soc.*, **91**, 1015-1057.

Shepard, D., 1968. A two-dimensional interpolation function for irregularly spaced data. Proceedings of the 1968 23rd ACM Natl. Conf., 517-524.

Shukla. J., 1998. Predictability in the midst of chaos: A scientific basis for climate forecasting. *Science*, **282**, 728-731.

Sikka, D. R., 2003. Evaluation of monitoring and forecasting of summer monsoon over India and a review of monsoon drought of 2002. *Proc. Indian Natl. Sci. Acad.*, **69**, 479-504.

Singh, S. V., et al., 1992: Interannual Variability of the Madden-Julian Oscillations in Indian summer monsoon rainfall. *J. Climate*, **5**, 973–978.

Suhas, E., and B. N. Goswami, 2008. Regime shift in Indian summer monsoon climatological intraseasonal oscillations. *Geophysical Research Letters*, **35**.

Trenberth, K. E., and C. J. Guillemot, 1998: Evaluation of the atmospheric moisture and hydrological cycle in the NCEP/NCAR reanalyses. *Climate Dyn.*, **14,** 213–231.

_____, K. E., 1999. Atmospheric moisture recycling: Role of advection and local evaporation. *J. Climate*, **12**, 1368–1381.

_____, K. E., et al., 2003. The changing character of precipitation. *Bull. Amer. Meteor. Soc.*, **9**, 1205–1217.

Vernekar, et al., 1995: The effect of Eurasian snow cover on the Indian nonsoon. *J. Climate*, **8**, 248–266.

BIOGRAPHICAL SKETCH

Peter Pantina was born in New Port Richey, FL on October 23, 1986, and became interested in science from an early age. He graduated as valedictorian of the International Baccalaureate Program at Land O' Lakes High School in 2005. He enrolled at the Harriet L. Wilkes Honors College at Florida Atlantic University in Jupiter, FL and graduated summa cum laude with a Bachelor's degree in Biological Sciences in 2008. Deciding to switch his course of action, he began his graduate education in meteorology at Florida State University in Tallahassee, FL. He was inducted into the Chi Epsilon Pi Honor Society in Spring 2010, after which he began his master's research under the direction of professor Vasu Misra. His research now focuses on monsoons and climate variability, but his interest in biology still exists and will be incorporated in future careers. In his spare time, he is an avid U.S. traveler, and had visited some fifteen national parks at the time of this composition. His three years in Tallahassee have influenced him in more ways than one.